

# Dual functional BAFF receptor aptamers inhibit ligand-induced proliferation and deliver siRNAs to NHL cells

Jiehua Zhou<sup>1</sup>, Katrin Tiemann<sup>1</sup>, Pritsana Chomchan<sup>1</sup>, Jessica Alluin<sup>1</sup>, Piotr Swiderski<sup>2</sup>, John Burnett<sup>1</sup>, Xizhe Zhang<sup>3</sup>, Stephen Forman<sup>4</sup>, Robert Chen<sup>4</sup> and John Rossi<sup>1,3,\*</sup>

<sup>1</sup>Department of Molecular and Cellular Biology, Beckman Research Institute of City of Hope, Duarte, CA 91010, USA, <sup>2</sup>Department of Molecular Medicine, Beckman Research Institute of City of Hope, Duarte, CA 91010, USA, <sup>3</sup>Irell and Manella Graduate School of Biological Sciences, Beckman Research Institute of City of Hope, Duarte, CA 91010, USA and <sup>4</sup>Department of Hematology and Bone Marrow Transplantation, City of Hope National Medical Center, Duarte, CA 91010, USA

Received December 13, 2012; Revised February 5, 2013; Accepted February 7, 2013

## ABSTRACT

The B-cell-activating factor (BAFF)-receptor (BAFF-R) is restrictedly expressed on B-cells and is often overexpressed in B-cell malignancies, such as non-Hodgkin's lymphoma. On binding to its ligand BAFF, proliferation and cell survival are increased, enabling cancer cells to proliferate faster than normal B-cells. Nucleic acid aptamers can bind to target ligands with high specificity and affinity and may offer therapeutic advantages over antibody-based approaches. In this study, we isolated several 2'-F-modified RNA aptamers targeting the B-cell-specific BAFF-R with nanomolar affinity using *in vitro* SELEX technology. The aptamers efficiently bound to BAFF-R on the surface of B-cells, blocked BAFF-mediated B-cell proliferation and were internalized into B-cells. Furthermore, chimeric molecules between the BAFF-R aptamer and small interfering RNAs (siRNAs) were specifically delivered to BAFF-R expressing cells with a similar efficiency as the aptamer alone. We demonstrate that a signal transducer and activator of transcription 3 (STAT3) siRNA delivered by the BAFF-R aptamer was processed by Dicer and efficiently reduced levels of target mRNA and protein in Jeko-1 and Z138 human B-cell lines. Collectively, our results demonstrate that the dual-functional BAFF-R aptamer-siRNA conjugates are able to deliver siRNAs and block ligand mediated processes, suggesting it might be a promising combinatorial therapeutic agent for B-cell malignancies.

## INTRODUCTION

The B-cell-activating factor (BAFF, also named Blys, TALL-1), a member of the tumour necrosis factor (TNF) family cytokines, has been shown to enhance the maturation and survival of peripheral B-cells (1–3). BAFF is produced by dendritic cells, monocytes and macrophages (4), and it binds to three receptors: the BAFF-receptor (BAFF-R), the transmembrane activator and calcium modulator and cyclophilin ligand interactor (TACI), and the B-cell maturation antigen (BCMA). Although BCMA and TACI also interact with other ligands, BAFF-R is exclusive to BAFF. BAFF trimerizes and binds to the BAFF-R on the cell surface where it is internalized by receptor-mediated endocytosis (5,6). Therefore, the interaction of BAFF and BAFF-R was identified as significant in B-cell survival, proliferation and maintenance (7–9). Excessive BAFF production triggers severe autoimmune disorders in mice resembling systemic lupus erythematosus and Sjögren's syndrome (10). Increased expression of BAFF and its receptors has also been identified in numerous B-cell malignancies (11–14), such as non-Hodgkin's lymphoma (NHL).

The American Cancer Society projects 70 000 new cases and 19 000 deaths in USA from NHL in 2012 (15). NHL comprises a heterogeneous group of lymphoid malignancies, which has important prognostic implications for the outcomes of treatments. Diffuse large B-cell lymphoma (DLBCL) is the most common type of NHL (16). Other lymphoma subtypes transform into DLBCL as they progress. Patients often respond well to treatments of chemotherapy or radiotherapy in combination with Rituximab (17). Nevertheless ~50% of DLBCL patients relapse within 2–3 years of treatment and require additional therapy, such as stem cell transplantation,

\*To whom correspondence should be addressed. Tel: +1 626 301 8360; Fax: +1 626 301 8271; Email: jrossi@coh.org

The authors wish it to be known that, in their opinion, the first two authors should be regarded as joint First Authors.

although that too is often not curative (17–20). Representing 6% of all NHL, Mantle cell lymphoma (MCL) is a relatively rare cancer. However, the clinical evolution of MCL is aggressive, with the lowest 5-year survival rate of any type of lymphoma, and is characterized with poor response to conventional therapeutic regimens (21). MCL is, therefore, considered an incurable malignancy and disease. It was demonstrated that NHL B-cell lines derived from patients express higher levels of BAFF than normal B-cells (11), and the BAFF-R is the most abundantly expressed in ~80% of MCLs and 40% of DLBCLs (22).

Constitutive expression of oncogenes, such as Bcl-2, c-Myc, signal transducer and activator of transcription 3 (STAT3), cyclins D1 and D2 and Syk, is a common feature among various subtypes of NHL, including MCL and DLBCL (23,24). Many of these are transcription factors, anti-apoptotic genes or genes involved in the cell cycle that are generated by reciprocal chromosomal translocation and mutations. When such genes are overexpressed, uncontrolled cell proliferation and survival of malignant cells ensues (25). Constitutive expression of the transcription factor STAT3 deregulates cell cycle progression, apoptosis, angiogenesis and tumour cell evasion of the immune system (26,27). The activated B-cell subgroups of DLBCL and MCL depend on constitutive activation of STAT3 for cell survival and proliferation (28,29). Furthermore, the expression and release of BAFF is regulated by JAK (Janus kinase)-STAT pathway, especially the STAT1- and STAT3-dependent signalling pathways. Further studies suggest that BAFF promotes *in vitro* and *in vivo* B-cell survival by upregulating anti-apoptotic proteins, such as Bcl-2 and Bcl-xL (30,31).

Knockdown of such oncogenes in B-cells by RNA interference (RNAi) may be a promising approach for treating B-cell lymphomas. RNAi is a conserved endogenous mechanism in which small interfering RNAs (siRNAs) suppress target-specific gene expression by promoting mRNA degradation. There are many potential uses for siRNAs in a clinical setting, for example, in developing therapeutic agents. However, there are several challenges in using siRNAs *in vivo*, including poor stability, potential for off-target effects and ensuring specific delivery to the correct tissue or cells. Nucleic acid aptamers (32) that target specific cell surface proteins have been used as delivery molecules to target a distinct cell type, hence, reducing off-target effect or other unwanted side effect (33,34). BAFF-R, restrictedly expressed on B-cell lines (35) including primary B-cells and mature peripheral B-cells, represents an attractive target for intervention in B-cell lymphomas and autoimmune diseases. To date, no one has attempted to identify aptamers that specifically recognize the BAFF-R.

In this study, we used the *in vitro* Systematic Evolution of Ligands by Exponential enrichment (SELEX) procedure to isolate several 2'-F-modified RNA aptamers against BAFF-R. We demonstrate that the evolved anti-BAFF-R aptamers with nanomolar affinity also efficiently bound and were specifically internalized to B-cells. Moreover, the anti-BAFF-R aptamers that did not

trigger B-cell proliferation were able to block BAFF ligand-mediated cell proliferation and compete effectively with BAFF ligand for receptor binding. In an effort to enhance the functional use of the aptamers, by using STAT3 as a proof of principle target, we created two different types of BAFF-R aptamer-STAT3 Dicer substrate siRNA (DsiRNA) conjugates for cell-type-specific siRNA delivery. One is covalent aptamer-siRNA chimera, and another is non-covalent aptamer-stick-siRNA conjugate. We demonstrated that the DsiRNA delivered by aptamers was processed by Dicer and incorporated in RISC (RNA-induced silencing complex) where it triggered potent knockdown of the STAT3 mRNA and protein in B-cell lines. Taken together, our results demonstrate that the dual-functional BAFF-R aptamers are able to deliver siRNAs as well as block ligand-mediated processes, suggesting that the aptamer-siRNA conjugates may represent a promising combinatorial nucleic acid-based therapeutics for B-cell malignancies.

## MATERIALS AND METHODS

### Materials

Unless otherwise noted, all chemicals were purchased from Sigma-Aldrich, all restriction enzymes were obtained from New England BioLabs (NEB) and all cell culture products were purchased from GIBCO (Gibco BRL/Life Technologies, a division of Invitrogen, Grand Island, NY, USA). Sources for the other reagents were DuraScribe T7 transcription Kit (EPICENTRE Biotechnologies, Madison, WI, USA); Silencer siRNA Labelling Kit (Ambion); Hoechst 33342 (Molecular Probes, Invitrogen, Grand Island, NY, USA); Random primers (Invitrogen); Bio-Spin 30 Columns (Bio-Rad, Hercules, CA, USA); Lipofectamine 2000 (Invitrogen); Human Embryonic Kidney 293 cells (HEK293), Rec-1 and CCRF-CEM cells (Human T cell lymphoblast-like cell line) (ATCC, Manassas, VA, USA); the BAFF-R protein (B-cell Activating Factor Receptor Human Recombinant, Cat # CYT-429), BAFF human (B-cell activating factor human Recombinant, CYT-307) and TNFRSF17 Human (B-cell maturation antigen human recombinant, BCMA, Cat # CYT-598) were obtained from ProSpect (East Brunswick, NJ, USA).

SiRNAs and sense or antisense strand of siRNAs were purchased from Integrated DNA Technologies (IDT, Coralville, IA, USA).

**STAT3-27 OVH DsiRNA (27/25-mer siRNA):** Sense: 5'-GAG AAC GGA AGC UGC AGA AAG AUA CGA-3' (27-mer); Antisense: 5'-GUA UCU UUC UGC AGC UUC CGU UCU C-3' (25-mer)

**STAT3-27 SWAP DsiRNA (25/27-mer siRNA):** Sense: 5'-GGA AGC UGC AGA AAG AUA CGA CUG a-3' (25-mer); Antisense: 5'-UCA GUC GUA UCU UUC UGC AGC UUC CGU-3' (27-mer).

### Generation of aptamer and chimera RNAs by *in vitro* transcription

Aptamer and chimera RNAs were prepared as previously described (33). The sense or antisense strands of siRNA in

the chimeras are underlined. Aptamer and sense or anti-sense strands of siRNA in the chimeras contain 2'-F-modified U and C. The italic *Us* are the linker between the aptamer and siRNA portions. The lowercases are DNA residues.

**R-1 aptamer:** 5'-GGG AGG ACG AUG CGG GAG GCU CAA CAA UGA UAG AGC CCG CAA UGU UGA UAG UUG UGC CCA GUC UGC AGA CGA CUC GCC CGA-3'

**R-14 aptamer:** 5'-GGG AGG ACG AUG CGG AUA ACU AUU GUG CUA GAG GGC UUA UUU AUG UGA GCC GGU UGA UAG UUG CGC AGA CGA CUC GCC CGA-3'

**R-22 aptamer:** 5'-GGG AGG ACG AUG CGG AUC CUC CGA AGG UCG CGC CAA CGU CAC ACA UUA AGC UUU UGU UCG UCU GCA GAC GAC UCG CCC GA-3'

**R-1-STAT3 27-mer Overhang (OVH) chimera sense strand:** 5'-GGG AGG ACG AUG CGG GAG GCU CAA CAA UGA UAG AGC CCG CAA UGU UGA UAG UUG UGC CCA GUC UGC AGA CGA CUC GCC CGA UUUUUUUU GAG AAC GGA AGC UGC AGA AAG AUA CGA-3'

**STAT3 27-mer OVH antisense strand:** 5'-GUA UCU UUC UGC AGC UUC CGU UCU C-3' (25-mer)

**R-1-STAT3 27-mer SWAP chimera antisense strand:** 5'-GGG AGG ACG AUG CGG GAG GCU CAA CAA UGA UAG AGC CCG CAA UGU UGA UAG UUG UGC CCA GUC UGC AGA CGA CUC CCC GA UUUUUU UCA GUC GUA UCU UUC UGC AGC UUC CGU-3'

**STAT3 27-mer SWAP sense strand:** 5'-GGA AGC UGC AGA AAG AUA CGA CUG a-3' (25-mer)

**R-1-CCND1 D-1 chimera sense strand:** 5'-GGG AGG ACG AUG CGG GAG GCU CAA CAA UGA UAG AGC CCG CAA UGU UGA UAG UUG UGC CCA GUC UGC AGA CGA CUC GCC CGA UU > CCA CAG AUG UGA AGU UCA UUU CCA A-3'

**CCND1 D-1 antisense strand:** 5'-UUG GAA AUG AAC UUC ACA UCU GUG GCA-3'

### Aptamer-stick-siRNA conjugates

R-1-stick, stick-sense and stick-antisense were chemically synthesized in the RNA synthesis facility of the City of Hope. The aptamer-stick-siRNA conjugates were prepared as previously described (36). Aptamer and sense strand contain 2'-F-modified U and C. The stick portion is underlined and contains 2'-OMe-modified A and G and 2'-F-modified U and C. The italic *X* indicates the three carbon linkers (C3) between the aptamer/siRNA and stick sequences. The lowercases are DNA residues.

**R-1-stick:** 5'-GGG AGG ACG AUG CGG GAG GCU CAA CAA UGA UAG AGC CCG CAA UGU UGA UAG UUG UGC CCA GUC UGC AGA CGA CUC GCC CGA XXXXXXXX GUA CAU UCU AGA UAG CC-3'

**Antisense-stick:** 5'-GUA UCU UUC UGC AGC UUC CGU UCU C XXXXX GGC UAU CUA GAA UGU AC-3'

**Sense strand:** 5'-gaG AAC GGA AGC UGC AGA AAG AUA CGA-3'

**Stick-sense:** 5'-GGA AGC UGC AGA AAG AUA CGA CUG A XXXXX GGC UAU CUA GAA UGU AC-3'

**Antisense strand:** 5'-uca GUC GUA UCU UUC UGC AGC UUC CGU-3'

### In vitro selection of RNA aptamers

The starting DNA library contained 50 nt of random sequences and was synthesized by Integrated DNA Technologies (Coralville, IA, USA). The random region is flanked by constant regions, which include the T7 promoter (underlined) for *in vitro* transcription and a 3'-tag for reverse transcription-polymerase chain reaction (RT-PCR). The 5' and 3' constant sequences are 5'-TAA TAC GAC TCA CTA TAG GGA GGA CGA TGC GG-3' (32-mer) and 5'-TCG GGC GAG TCG TCT G-3' (16-mer), respectively. The DNA random library (0.4 μM) was amplified by PCR using 3 μM each of 5'- and 3'-primers, along with 2 mM MgCl<sub>2</sub> and 200 μM of each dNTP. To preserve the abundance of the original DNA library, PCR was limited to 10 cycles. After the PCR reactions (10 reactions, 100 μl per reaction), the amplified dsDNA pool was recovered using a QIAquick Gel purification Kit. The resulting dsDNA was converted to an RNA library using the DuraScript Kit (Epicentre, Madison, WI, USA) according to the manufacturer's instructions. In the transcription reaction mixture, CTP and UTP were replaced with 2'-F-CTP and 2'-F-UTP to produce ribonuclease resistant RNA. The reactions were incubated at 37°C for 6 h, and subsequently the template DNA was removed by DNase I digestion. The transcribed RNA pool was purified in an 8% polyacrylamide/7 M urea gel. The purified RNA library was quantified by ultraviolet spectrophotometry.

The SELEX was performed principally as described by Tuerk and Gold (37), and the details were described previously (36). In each round, the RNA pools were refolded in HBS buffer (10 mM HEPES, pH 7.4, 150 mM NaCl, 1 mM CaCl<sub>2</sub>, 1 mM MgCl<sub>2</sub> and 2.7 mM KCl), heated to 95°C for 3 min and then slowly cooled to 37°C. Incubation was continued at 37°C for 10 min. Generally, to minimize non-specific binding with the nitrocellulose filters, the refolded RNA pools were pre-adsorbed to a nitrocellulose filter (HAWP filter, 0.45 μm) for 30 min, before incubation with the human BAFF-R protein. The pre-cleared RNA pool was incubated with the target protein in low-salt RNA-binding buffer (10 mM HEPES, pH 7.4, 50 mM NaCl, 1 mM CaCl<sub>2</sub>, 1 mM MgCl<sub>2</sub>, 2.7 mM KCl, 10 mM Dithiothreitol (DTT) and 0.01% bovine serum albumin and tRNA) for 30 min for SELEX rounds 1-4. After the fourth round of SELEX, a high-salt RNA-binding buffer (10 mM HEPES, pH 7.4, 150 mM NaCl, 1 mM CaCl<sub>2</sub>, 1 mM MgCl<sub>2</sub>, 2.7 mM KCl, 10 mM DTT and 0.01% bovine serum albumin and tRNA) was used. With the SELEX progress, the amount of BAFF-R protein was reduced, and competitor tRNA was increased to increase the stringency of aptamer selection.

For the first cycle of selection, the pre-cleared random RNA pool (73.26 μg, 2.6 nmol, 1.5 × 10<sup>15</sup> molecules) and

human BAFF-R protein (0.65 nmol, RNA/protein ratio 4/1) were incubated in 200  $\mu$ l low-salt RNA-binding buffer on a rotating platform at room temperature for 30 min. The reaction was passed through a pre-wetted nitrocellulose filter and washed with 1 ml of binding buffer. The bound RNA was eluted from the filter with 200  $\mu$ l of elution buffer (7 M urea and 5 mM ethylenediaminetetraacetic acid) at 95°C for 5 min, followed by phenol/chloroform extraction and concentration with a Microcon YM-30 column. The recovered RNA pool was reverse transcribed using the ThermoScript RT-PCR system (Invitrogen) and amplified for 15 cycles of PCR. After the amplified dsDNA pool was purified using a QIAquick Gel purification Kit, it was transcribed as described previously for the next round of selection.

After 11 and 12 rounds of SELEX, the resulting cDNAs were amplified by PCR and cloned into the TOPO TA cloning vector pCR<sup>®</sup>2.1-TOPO (Invitrogen). Individual clones were identified by DNA sequencing.

#### Filter-binding assays

Filter-binding assays were used to detect the binding affinity of the individual aptamers. The RNAs were treated with CIP (calf intestinal phosphatase), removing the initiating 5'-triphosphate and labelled with  $\gamma$ -<sup>32</sup>P-adenosine triphosphate by T4 polynucleotide kinase. The end-labelled RNA (2 nM) was incubated with BAFF-R protein (100 nM) and a 10-fold molar excess of non-specific competitor tRNA (20 nM) in the RNA-binding buffer for 30 min. In all, 100  $\mu$ l of binding reaction was separated by a pre-wet nitrocellulose filter. After washing the filter with 2 ml of binding buffer, the radioactivity retained on the filter was counted by a multi-purpose scintillation counter (Beckman Coulter). The binding affinity was obtained by calculating the per cent of the RNA retained on the filter in the input RNA.

#### Cell culture

Rec-1 cells were purchased from ATCC and cultured in RPMI 1640 supplemented with 10% FBS and 1% glutamine. CEM cells were purchased from ATCC and cultured in Dulbecco's modified Eagle's medium supplemented with 10% FBS. Jeko-1, Z138 and Grant-519 cells were kindly provided by Dr Robert Chen, City of Hope and were sustained in RPMI 1640 medium supplemented with 20% FBS (Jeko-1) or 10% FBS and 1% glutamine. Cells were cultured in a humidified 5% CO<sub>2</sub> incubator at 37°C.

#### Internalization studies (live-cell confocal microscopy analyses)

On the day of the experiments, the Jeko-1, Z138 or CCRF-CEM cells were seeded in the polylysine-coated 35-mm plate (Glass Bottom Dish, MatTek, Ashland, MA, USA) with seeding at  $8 \times 10^5$  in the pre-warmed RPMI-1460 medium. Cells were incubated for 0.5–1 h in a humidified 5% CO<sub>2</sub> incubator at 37°C for attaching on the dish surface. Cy3-labelled RNAs at a 66 nM final concentration were added to media and incubated for live-cell confocal microscopy in a 5% CO<sub>2</sub> microscopy incubator

at 37°C. The images were collected every 15 min using a Zeiss LSM 510 Meta Inverted two photon confocal microscope system under water immersion at 40 $\times$  magnification. After 5 h of incubation and imaging, the cells were stained by treatment with 0.15 mg/ml of Hoechst 33342 (nuclear dye for live cells, Molecular Probes, Invitrogen) according to the manufacturer's instructions. The images were collected as described previously.

#### Cell proliferation (MTS assay)

A total of  $6 \times 10^4$  Jeko-1, Z138, Granta 519 or Rec-1 cells were seeded into 96-well plates. Cells were incubated with increasing concentrations (0, 50, 100, 200 and 400 nM) of BAFF-R aptamers (R-1, R-14 and R-22), chimeras (R-1-STAT3 27-mer OVH and R-1-STAT3 27-mer SWAP chimeras), R-1-stick-STAT3 siRNA conjugates (STAT3 N-1 and N-2) or BAFF ligand (Prospec-Tany TechnoGene Ltd, East Brunswick, NJ, USA). At 48 h post-treatment, CellTiter 96<sup>®</sup> Non-Radioactive Cell Proliferation (Promega) assays were performed according to manufacturer's protocol. Experiments were performed in triplicate.

#### MTS competition assay

A total of  $6 \times 10^4$  Rec-1 or Z138 cells were seeded into 96-well plates. Cells were incubated either with BAFF-R aptamers or BAFF ligand in increasing concentrations (50, 100, 200 and 400 nM) as controls or with 200 nM BAFF ligand (Prospec-Tany TechnoGene Ltd) and increasing concentrations of R-1 or R-14 aptamer (50, 100, 200 and 400 nM). The MTS was performed as described earlier in the text. Experiments were performed in triplicate.

#### Electroporation of siRNA

A concentration of  $4 \times 10^6$  cells/ml and 200 nM of siRNAs were used for electroporation by Bio Rad's Gene Pulser MXcell Electroporator. Gene pulser electroporation buffer along with 24-well electroporation plates were used also from Bio Rad. The electroporation condition was set-up as (i) exponential waveform; (ii) 200 V; (iii) 350 mf (capacitance) and (iv) resistance of 1000. After electroporation, 0.5 ml of electroporated cells were transferred to a 6-well plate containing 2-ml medium of RPMI-1640 immediately.

#### Cell apoptosis by flow cytometry assay

Jeko-1 cells were seeded in duplicate at a density of  $8 \times 10^5$  cells/ml into 24-well plates. Cells were treated with aptamer or electroporation with siRNA. Cells were harvested and stained with annexin V-FITC and propidium iodide (BD Pharmingen) and assessed for the percentage of double-negative population using an Accuri C6 flow cytometer. Apoptosis data were analysed using FlowJo version 7.6.1 software (TreeStar).

### RNA extraction and quantitative RT-PCR analysis of STAT3 mRNA

A total of  $2 \times 10^5$  cells (Jeko-1, Z138 and CCRF-CEM) were treated directly with the experimental RNA (400 nM). After 2 or 4 days of incubation, total RNAs were isolated with STAT-60 (TEL-TEST, Friendswood, TX, USA) according to the manufacturer's instructions (Tel-Test). Residual DNA was digested using the DNA-free kit per the manufacturer's instructions (Ambion, CA, USA). cDNA was produced using 2  $\mu$ g of total RNA Moloney murine leukaemia virus reverse transcriptase and random primers in a 15- $\mu$ l reaction according to the manufacturer's instructions (Invitrogen, CA, USA). Expression of the *STAT3* coding RNAs was analysed by quantitative RT-PCR using 2 $\times$  iQ SyberGreen Mastermix (BIO-RAD) and specific primer sets at a final concentration of 400 nM. Primers were as follows: STAT3 forward primer: 5'-GCA GGA GGG CAG TTT GAG-3'; STAT3 reserved primer: 5'-CGC CTC AGT CGT ATC TTT CTG-3'; GAPDH forward primer: 5'-CAT TGA CCT CAA CTA CAT G-3'; GAPDH reverse primer: 5'-TCT CCA TGG TGG TGA AGA C-3'. GAPDH expression was used for normalization of the qPCR data. Quantitative RT-PCR (qRT-PCR) reactions were amplified as described earlier in the text.

### Protein extraction and western blot analysis

Protein extraction was performed 48 h post-incubation by adding 50–100  $\mu$ l of M-Per<sup>®</sup> Mammalian Protein Extraction Reagent lysis buffer (Thermo Scientific), containing Complete, Mini Protease Inhibitor Cocktail (Roche). Samples were frozen in an ethanol bath for 30 s and thawed for 30 s in a 37°C water bath, repeating freeze thaw cycles twice followed by centrifugation at 13 000 rpm for 10 min at 4°C. The concentration of the samples was determined with the Bio-Rad Protein Assay according to manufacturer's instructions. Samples were stored at –80°C until assay.

Proteins (25  $\mu$ g) were separated on a 12% sodium dodecyl sulphate–polyacrylamide gel electrophoresis. Immunoblotting identified STAT3 and  $\alpha$ -tubulin proteins. STAT3 (86 kDa) with rabbit anti-STAT3 IgG from Santa Cruz Biotechnology and the loading control  $\alpha$ -tubulin (55 kDa) were detected with mouse anti- $\alpha$ -tubulin IgG from Sigma-Aldrich and goat anti-mouse IgG-HRP or anti-rabbit-IgG-HRP (Santa Cruz Biotechnology) as secondary antibodies.

### Selectin L (SELL) mRNA expression detected by quantitative RT-PCR

Total RNA was reverse-transcribed into complementary DNA (cDNA) with iScript Reverse Transcriptase Supermix (Bio Rad, Hercules, CA, USA) according to manufacturer's specifications (Bio Rad, Hercules, CA, USA). One RNA sample of each preparation was processed without RT to provide a negative control in subsequent RT-PCR reactions. Quantitative analysis of Selectin L (SELL) expression was performed by RT-PCR SYBR Green I (Bio Rad) analysis (C1000

Thermal Cycler, Bio Rad, Hercules, CA, USA). SELL expression was detected using 50 ng of cDNA, amplified with primer set SELL-forward (5'-TCA CGT CGT CTT CTG TAT ACT GTG G-3'), SELL-reverse (5'-TTG CAG CTA GCA TTT CAG TGA TG-3'). Internal control, human large ribosomal protein (RPLPO) expression was detected using 50 ng of cDNA, with primer set RPLPO-forward (5'-GGC GAC CTG GAA GTC CAA-3') and RPLPO-reverse (5'-CCA TCA GCA CCA CAG CCT TC-3'). SELL and RPLPO PCR reactions were amplified using PCR conditions of 95°C for 5 min, followed by 40 cycles of 95°C for 30 s, 59°C for 1 min and 72°C for 1 min.

## RESULTS

### Selection and identification of RNA aptamers against human BAFF-R protein

The 2'-Fluoropyrimidine-modified RNA aptamers that selectively bind to recombinant human BAFF-R protein were selected using an *in vitro* SELEX procedure (36). Filter-binding assays monitored the progress of selection after each SELEX cycle (Supplementary Figure S1A). The binding affinity was evaluated as the per cent of the RNA retained on the filter in the total RNA pool. When compared with the second round RNA pool (2-RNA), in which 1.6% of the input RNAs were retained on the membrane, the 10th RNA library (10-RNA) had 12.1% of the input RNA bound. After the 11th round of selection, no further enrichment could be detected (Supplementary Figure S1A), suggesting that maximal binding of the RNA pool had been reached. The binding activities of the RNA pools were further confirmed by gel shift assays (Supplementary Figure S1B). These results indicated that the RNA pool was successively enriched in aptamers with high-binding affinity for the target protein.

The highly enriched aptamer pools (11-RNA and 12-RNA) were cloned into TOPO TA cloning vector and sequenced. The individual clones were classified into 11 different groups based on the alignments of individual aptamer sequences (Table 1). Approximately 28% of the clones (Group 1 aptamers) included conserved sequences, including seven nucleotides (GAGGCUC), which are underlined in Table 1. No common secondary structural motifs in these groups were observed using secondary structure predictions based on the RNA folding algorithms (Mfold and Quickfold) (Supplementary Figure S1C). One representative sequence from each group (R-1 to R-22) was chosen for further characterization because of their relative abundance within their group. Filter-binding assays confirmed the binding activity of these individual aptamers (Figure 1A). R-1, R-2 and R-14 aptamers showed the strongest binding affinities of >36% comparable with SELEX round 11, whereas R-22 illustrated the lowest binding affinity (3.6%) (Figure 1A).

Moreover, the dissociation constants ( $K_d$ ) for selected aptamers with the target protein were calculated from a native gel mobility shift assay (Figure 1B and Supplementary Figure S1D). Three of the aptamers exhibited effective binding kinetics to BAFF-R protein. The apparent  $K_d$  values of R-1, R-2 and R-14 were about

Table 1. The alignment and identification of BAFF-R RNA aptamers

Groups	Fixed sequence GGGAGGACGAUCCGG		Frequency (170 sequences) of BAFF-R pool	Fixed sequence CAGACGACUCGCCGA
Group 1 Total 43 25.2%	Conserved domain:  GAGGCUC 27.8%	R-1	<u>GAGGCUC</u> AACAAUGAUAGAGCCCGCAUGUUGAUAGUUGGCCAGUCUG	19 (11.2%)
		R-2	<u>GAGGCUC</u> GGCUUAGUAAGUAAAGAUUGAGCCCGCAUGACGCUCGAGUGC	5 (2.9%)
		R-3	G <u>GAGGCUC</u> UUAGAGCCUGCAUCUUGGAAAAGAUAAAGCCCGUGCAC	4 (2.4%)
		R-4	<u>GAGGCUC</u> GUGGAUGUUUAUCGAAAGAGCCCGCAAUCCGGUUGUCUGGUG	4 (2.4%)
		R-5	<u>GAGGCUC</u> GGUCAUUAAGGGUACUGAAAGCCCGGUCGGUUGUCUGGUG	1
		R-6	<u>U</u> GAGGCUCAUAGAGCACCGCAAAGAUAGAAAGUUGUUGCCAUCGAUAGUG	5 (2.9%)
		R-7	<u>U</u> GAGGCUCGAUUAGAGGUUGGUCUCUUGUGAGCCCGUAUCGCGAAUGCUG	1
		R-8	UUU <u>GAGGCUC</u> GCGACUACGAAGACAAACCGUAUCGCGUUGCAUCAUGGA	4 (2.4%)
Group 2 Total 26 15.3%	UUUCCC/ GGCGUCC	R-9	CAGGU <u>U</u> UCCC <u>GU</u> UUGUCGGUCAAACGGCGUCCGUUAGUUGGUGUG	14 (8.2%)
		R-10	<u>UUUCCC</u> CGGCCAAGUAGCUGGGCGUCCCGCAUUCUCACAGGACCGUACGCCG	11 (6.5%)
		R-11	<u>UUUCCC</u> UAGGAUCACAUCCGAUCUUAGGGCGUCCCGCACAGUCAACCCUGG	1
Group 3 Total 7	AAUCGC(C )G(U)AAU	R-12	<u>AAUCGC</u> CGAAU <u>GAGGCUC</u> UUAGAGCAUUCGGCGCGCAAACGAGCACGC	4 (2.4%)
		R-13	UC <u>AAUCGC</u> GUAAUAAACCGUUUGUGAACUGAUCUAAUCCGGUCUGAGGUG	3 (1.8%)
Group 4 Total 6	AUA(G)AC U	R-14	<u>AUAACU</u> AUUGUCUAGAGGGCUU <u>UUU</u> AUGUGAGCCGUUGAUAGUUGCG	5 (2.9%)
		R-15	<u>AUGACU</u> GACAGGGACUUCUUGGCA <u>UUU</u> UGCUGCGAGUUCACGGUGGCGC	1
Group 5		R-16	UUUACUGACCGUUUUGUAGGUUGGUAGCCUUGCUUCACAAGAAGUGUGCG	6 (3.5%)
Group 6		R-17	GACUUAGAUGCAGCGUUGUAUAAUCCGGUCGUCCUCUGGUACGUACGCGUG	2
Group 7		R-18	GAUAGGACAUAGCGAU <u>UCCC</u> GUUGUUUACGGUCGUUACUCAGGUCUGGC	2
Group 8		R-19	UUGAUUGUAAGAAUUGUGCAUAAAGGCAUUUACCCUUCUAGCAACGUGGAC	3 (1.8%)
Group 9		R-20	CUUAUGGUCUUUUAUUUUUUUUUUUUUCGACCCGCGGUGUCUUGGUCUGC	2
Group 10	UGUCCG	R-21	<u>UGUCCG</u> AAUCUCGAGAAACGGGAUUC <u>CGCUGCCG</u> GUCAUGUGUAGUUGGU	3 (1.8%)
Group 11	AUCC	R-22	<u>AUC</u> CUCGAAAGGUCGCGCCAACGUCACACAUAAGCUUUUGUUCGUCUG	2
Others			Orphan sequences	68

After the 12th round of selection, the selected RNA pool was cloned and sequenced. After alignment of all 170 clones, 11 groups of anti-BAFF-R aptamers were identified. Only the random sequences of the aptamer core regions (5'-3') are indicated. Isolates occurring with multiple frequencies are specified. Sequenced aptamers were grouped by conserved nucleotide stretches underlined in this table. Group 1 had the highest frequency among all sequenced aptamers.

47 nM, 95 nM and 96 nM (Figure 1B), respectively. Additionally, in gel shift competition with cold aptamers, the inhibition of all three aptamers was dose-dependent, suggesting the binding affinity of aptamers is specific to their target protein (Supplementary Figure S2A-C). As expected, the aptamer with the highest binding affinity (R-1) also had the strongest inhibition potential, followed by R-14 for all three tested aptamers (Supplementary Figure S2A-C). Furthermore, the specificity of selected aptamer binding to its target BAFF-R was confirmed by comparing its binding with that of the other TNF receptor protein (TNFRSF17 human, known as BCMA) and an irrelevant protein (HIV-1 gp120 protein). Gel shift assay revealed a strong affinity of R-1 for BAFF-R (Supplementary Figure S1D), whereas no binding was detectable for BCMA and gp120 protein (Supplementary Figure S2D). These results collectively indicate that the R-1 aptamer specifically recognizes BAFF-R in a high-affinity manner.

#### BAFF-R aptamers specifically bind and are internalized by BAFF-R expressing cells

Various B-cell lines derived from MCL (human Mantle cell lymphoma) were screened for their BAFF-R

expression level by western blot analysis and flow cytometry to choose an appropriate cell line as model cell for the function studies of BAFF-R aptamers, such as binding, internalization and siRNA delivery. As shown in Supplementary Figure S3A and B, Jeko-1 showed the highest BAFF-R level among the tested cells. Hence, further experiments were conducted with Jeko-1 cells.

First, Jeko-1 cells were tested for binding and internalization of two selected BAFF-R aptamers (R-1 and R-14) with CCRF-CEM cells (a human T-cell lymphoblast-like cell line) as a negative control. The BAFF-R aptamers were labelled with Cy3 to evaluate their binding and cellular uptake. Flow cytometric analysis (Supplementary Figure S3C) revealed that the R-1, R-2 and R-14 aptamers specifically bound to the BAFF-R expressing Jeko-1 cells but did not bind to the control CEM T-cells. As anticipated, non-binding R-22 aptamer and an irrelevant HIV-1 gp120 aptamer did not show binding specificity and had only less 10% background signals.

To determine whether the bound aptamers were internalized, we carried out real-time live-cell Z-axis confocal microscopy with R-1 (Figure 2A) and R-14 (Figure 2B) in Jeko-1. At 20 min post-incubation, the Cy3-labelled R-1 aptamers were promptly internalized

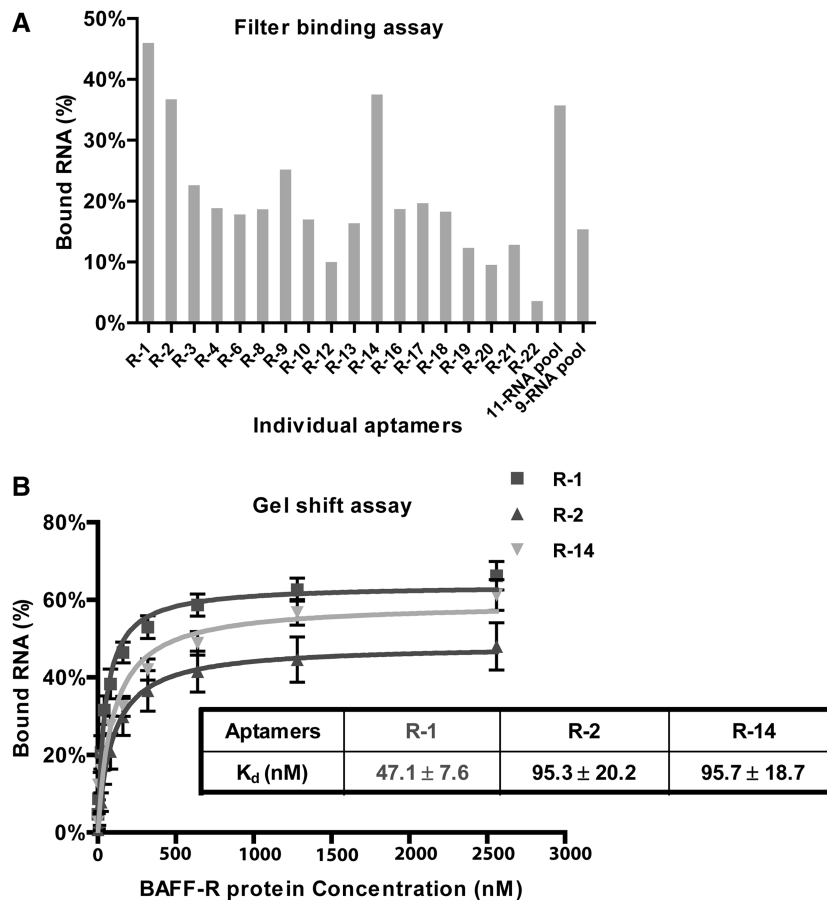


**Figure 1.** Binding of selected individual BAFF-R aptamers. (A) Nitrocellulose membrane filter binding assay. The 5'-end <sup>32</sup>P-labelled individual aptamers were incubated with the BAFF-R protein. The binding reaction mixtures were analysed by a filter-binding assay. Aptamer R-1, R-2 and R-14 showed the best binding affinity with the target protein. The bound RNA (y-axis) is illustrated in percentage. (B) Binding curve from a gel shift assay. The 5'-end <sup>32</sup>P-labelled individual aptamers were incubated with the increasing amounts of BAFF-R protein. The binding reaction mixtures were analysed by a gel mobility shift assay, and the calculated K<sub>d</sub> determinations are indicated.

by Jeko-1 cells, but not by the CCRF-CEM control cells (Figure 2C). We also used HIV-1 gp120 aptamer as an irrelevant control to determine the binding specificity. As shown in Supplementary Figure S3D and E, Cy3-labelled gp120 did not bind to B-cell chronic lymphocytic leukaemia (B-CLL), whereas R-1 aptamer was specifically internalized by B-CLL. To visualize the nucleus, the cells were stained with the nuclear dye Hoechst 33342 before incubation with the Cy3-labelled aptamer. The aptamer aggregated within the cytoplasm (Figure 2D), suggesting that the BAFF-R aptamers may enter cells *via* receptor-mediated endocytosis. A detailed mechanism remains still unclear, and further investigation is required.

#### BAFF-R aptamers block BAFF ligand-mediated cell proliferation

In a previous study, investigators demonstrated that BAFF trimerizes and binds to the BAFF-R on the cell surface where it is internalized by receptor-mediated endocytosis (5,6). This pathway enhances cell survival and cell proliferation of B-cells, which can cause autoimmune disease and cancer (38). Various B-cells derived from MCL, such as Jeko-1, Z138, Rec-1 or Granta-519 cells,

were incubated with increasing concentrations of BAFF-R aptamers (R-1 and R-14), a non-binding R-22 aptamer or BAFF ligand. After 48 h of post-treatment, the cells were analysed by MTS assay to measure B-cell proliferation (Figure 3A–D). BAFF ligand enhanced cell proliferation by 40% in Rec-1 cells (Figure 3B). In Jeko-1 and Granta-519, the increase in proliferation with BAFF ligand was less prevalent (Figure 3A and D). In Z138 cells, BAFF ligand induced no proliferation increase (Figure 3C). The variation of different B-cell lines, such as different BAFF-R level and cell doubling properties, probably did not behave in the same manner, thus resulting in different proliferative responses to the interaction of BAFF ligand/BAFF-R. However, all tested cell lines treated with aptamers R-1 and R-14 reduced cell proliferation.

In addition, an MTS competition assay was performed by treating Rec-1 cells (the highest increase in proliferation with BAFF ligand in our experiment) and Z138 (the lowest/no increase in proliferation) with a constant concentration of BAFF ligand and increasing concentrations of R-1 and R-14 aptamers. As shown in Figure 3E and F, the tested BAFF-R aptamers efficiently blocked BAFF ligand-mediated proliferation in Rec-1 and Z138

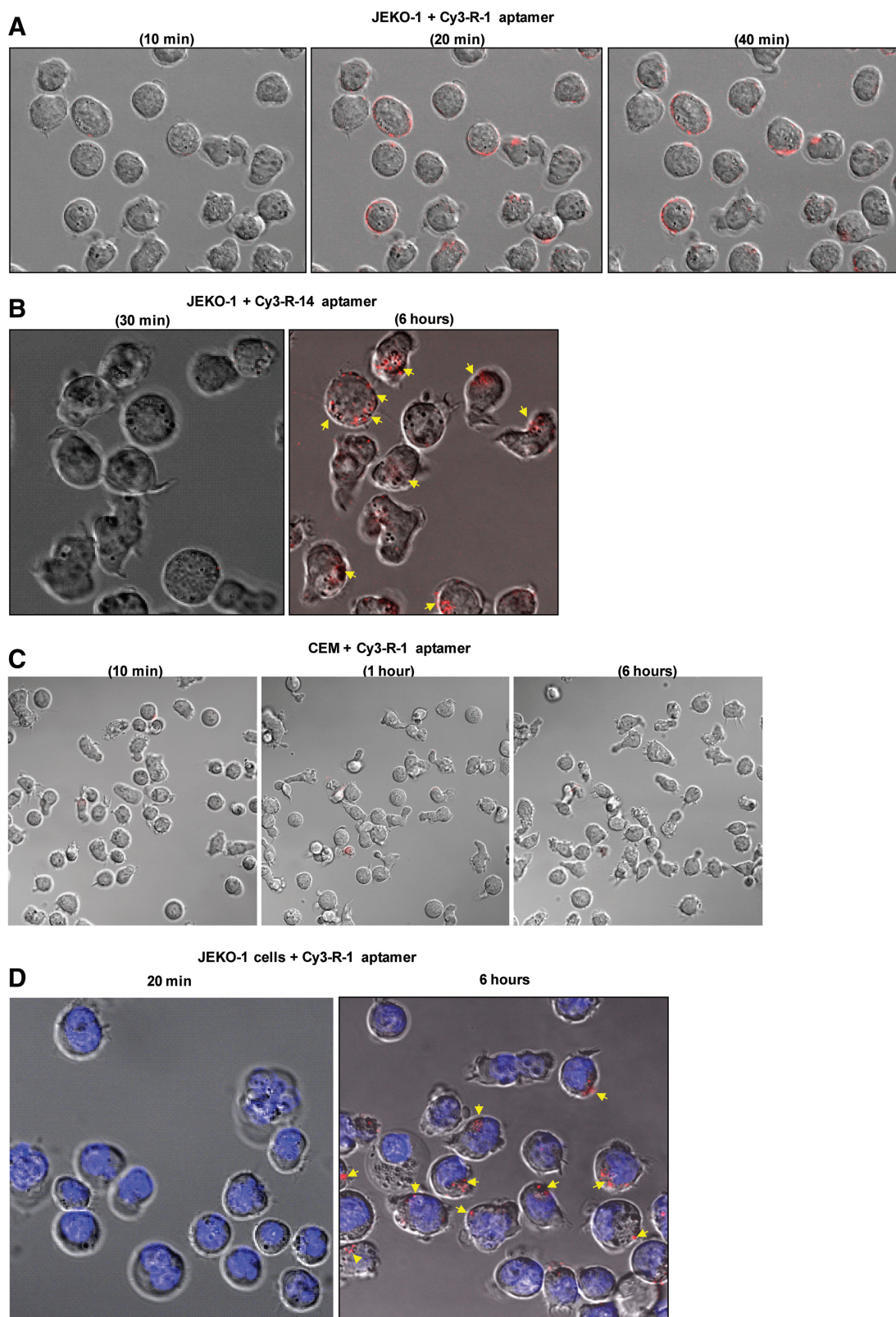


**Figure 2.** Cell-type-specific binding and uptake studies of aptamers. (A–C) Internalization analysis. Cy3-labelled RNAs were tested for binding to Jeko-1 cells (A, B) and CEM control cells (C). Cells were grown in 35-mm plates and incubated with a 60 nM concentration of Cy3-labelled aptamers in culture media for real-time live-cell-confocal microscopy analysis. The images were collected at 15-min intervals at 40× magnification. The selected aptamers (A, C) R-1 and (B) R-14 showed cell-type-specific binding affinity. (D) Localization analysis. Jeko-1 cells were grown in 35-mm plates. Before incubation with 60 nM of Cy3-labelled R-1, cells were stained with Hoechst 33342 (nuclear dye for live cells) and then analysed using real-time confocal microscopy.

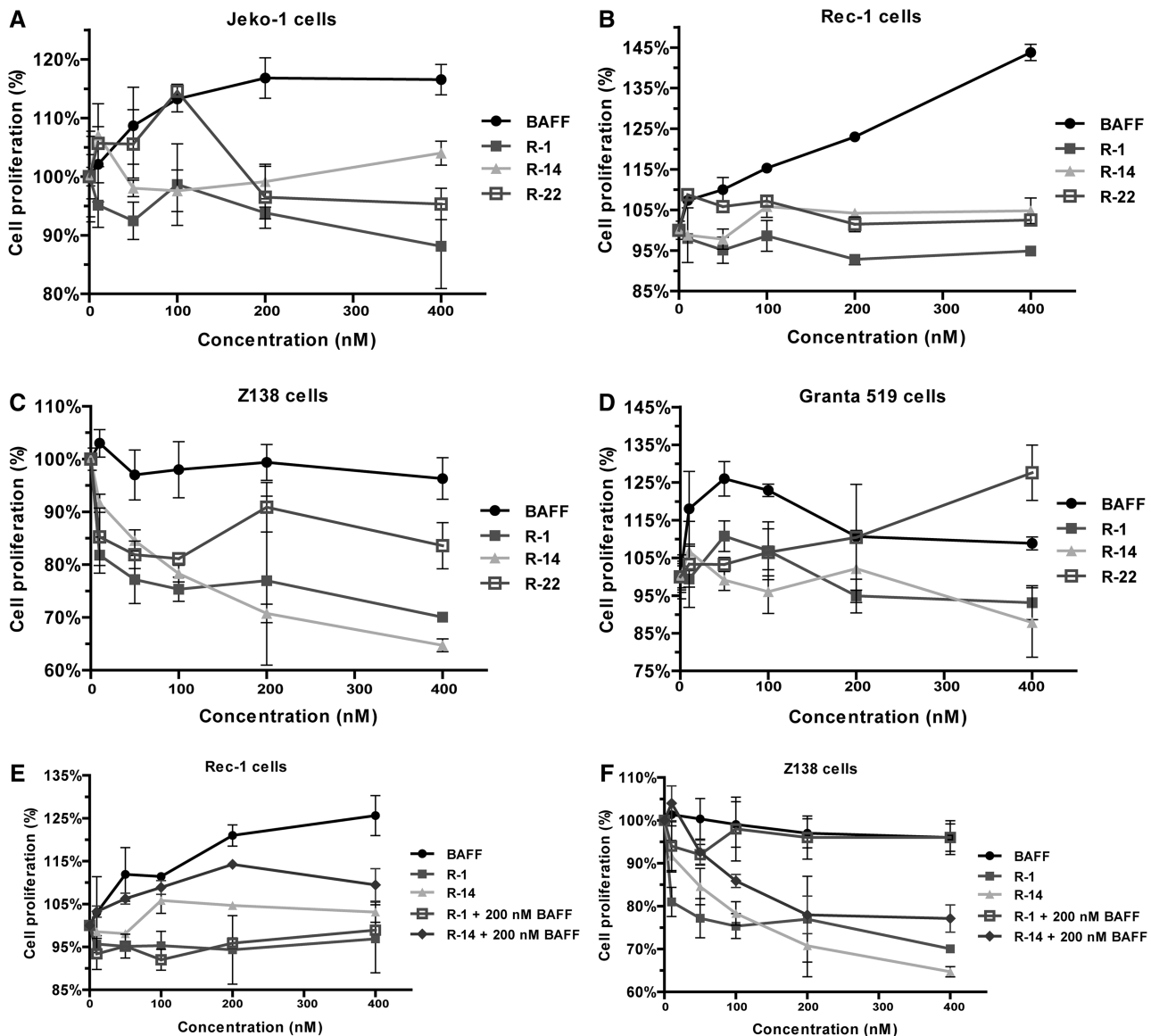


**Figure 3.** Proliferation and competition of aptamer-treated NHL cell lines. BAFF ligand can increase cell proliferation on binding to BAFF-R on B-cells. MTS assays were performed (A–F) to measure cell proliferation. Jeko-1 (A), Rec-1 (B), Z138 (C) and Granta-519 (D) cells were treated with increasing amounts of BAFF-R aptamers R-1, R-14 and R-22 or BAFF ligand. On 48 h post-incubation, MTS assays were performed, and cell proliferation was calculated in percentage and showed. (E–F) Cell proliferation was measured by MTS in Rec-1 (E) and Z138 (F) cells when treated with BAFF and increasing amounts of either R-1 or R-14 aptamers to investigate the potential of aptamers to block ligand-mediated proliferation.

cells. No further increase in proliferation than BAFF ligand alone could be detected in both cell lines treated with BAFF-R aptamers. A competitive gel shift assay was further performed to confirm the competition of aptamer and BAFF ligand to BAFF-R protein (Supplementary Figure S4). Our results showed that BAFF-R aptamers R-1 and R-14 were able to compete with BAFF ligand for BAFF-R protein in a dose-dependent manner.

#### Design of BAFF-R aptamer–siRNA chimera delivery systems that bind and are internalized by cells expressing BAFF-R

We next asked whether our selected aptamers could be used as cell-specific delivery vehicles for siRNAs. The

signal transducer and activator of transcription (STAT) proteins comprise of a family of transcription factors that regulate diverse cellular events, such as differentiation, proliferation and cell survival (27). The transcriptional targets of STAT proteins play roles in cell cycle progression and also cell survival (39). Constitutively active STATs, such as STAT3 and STAT5, contribute to a malignant phenotype in human cancer cell lines and primary tumours (40). In particular, STAT3 plays a crucial role in promoting progression of human cancers, including several types of B-cell lymphoma (26,27). It was demonstrated that downregulation of STAT3 activity can cause growth inhibition of the lymphoma tumour-cells *in vitro* and *in vivo* (27,39). In this regard, we, therefore, chose human STAT3 as model siRNA target gene.

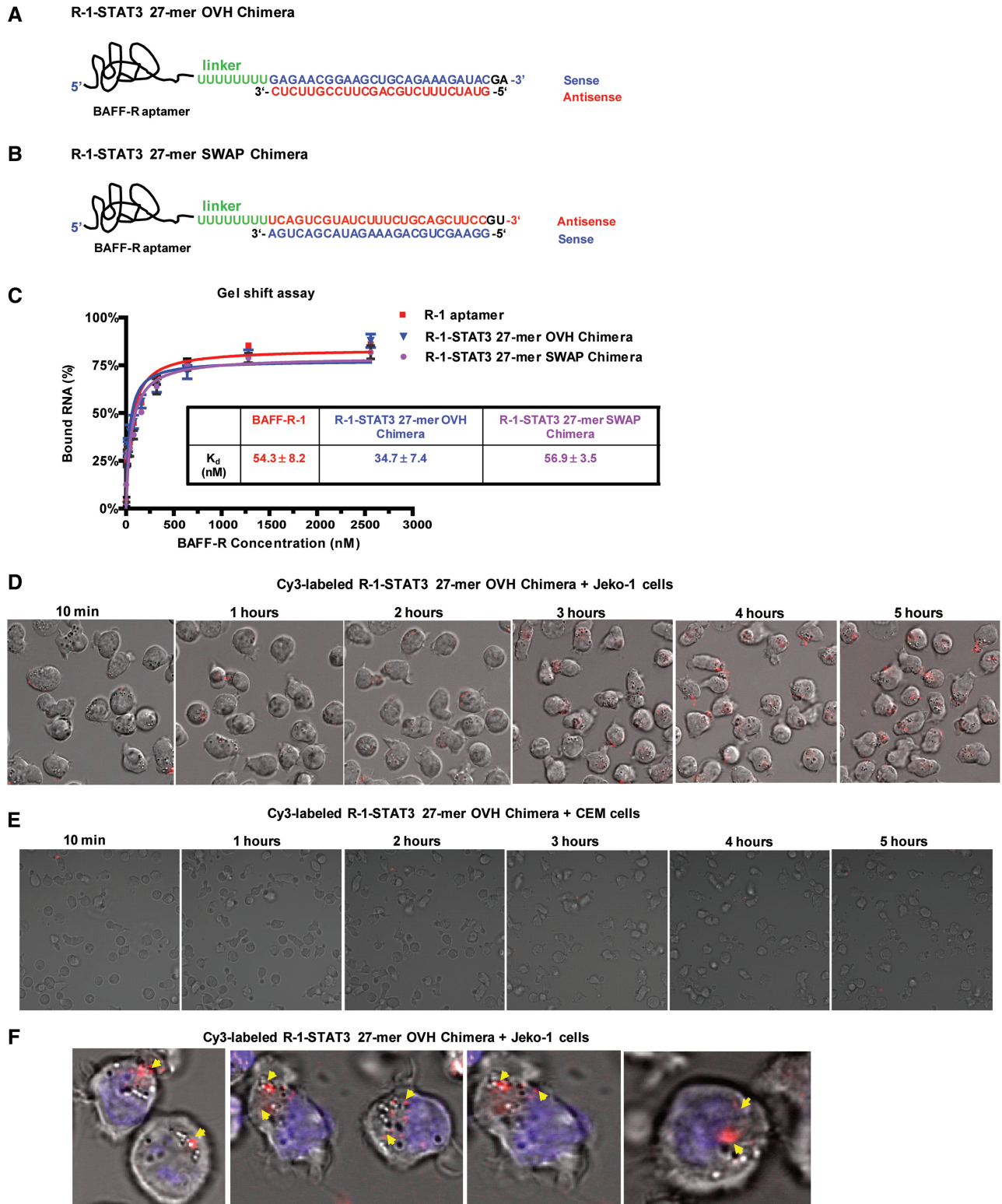


**Figure 4.** The design and binding affinity of aptamer–siRNA chimeras. (A and B) Schematic aptamer–siRNA chimeric RNAs: the region of the anti-BAFF-R aptamer is responsible for binding to BAFF-R, and the siRNA is targeting STAT3 gene. A linker (8U) between the aptamer and siRNA is indicated in green. Two versions, R-1-STAT3 27-mer OVH chimera (A) and R-1-STAT3 27-mer SWAP chimera (B), were designed, in which DsiRNA orientation is different. (C) Binding curve from a gel shift assay. The aptamer–siRNA chimeric RNAs that have comparable  $K_d$  values, as well as parental aptamers specifically bind the human BAFF-R protein. Data represent the average of three replicates. (D–F) Internalization and intracellular localization analyses. Jeko-1 (D) or CEM control cells (E) were grown in 35-mm plates and incubated in culture medium with a 60 nM concentration of chimeras containing a 5'-Cy3-labelled sense strand for real-time live-cell confocal microscopy analysis as previously described. The chimeras showed cell-type-specific binding affinity. (F) Localization study. After 5 h incubation, cells were stained with Hoechst 33342 (nuclear dye for live cells) and then analysed by confocal microscopy. The chimeras were localized in the cytoplasm of cells.

Herein, two aptamer–siRNA chimeras (R-1-STAT3 27-mer OVH chimera and 27-mer SWAP chimera) were designed and prepared as previously described (36,41) (Figure 4A and B). An eight nucleotide linker (8Us) was inserted between the aptamer portion and the anti-STAT3 DsiRNA portion to increase molecular flexibility for correct folding of the aptamer and for Dicer processing of DsiRNA. A 2-nt 3'-overhang was designed in the DsiRNA portion to facilitate Dicer binding and entry. We also swapped antisense and sense strand of the DsiRNA portion in the 27-mer SWAP design (Figure 4B), which is expected to readily incorporate the antisense strand into RISC.

Next, the binding affinities of the chimeras for BAFF-R protein were assessed by gel shifts assay as previous described. These data (Figure 4C and Supplementary Figure S5A) indicate that the two chimeras (27-mer OVH chimera: 35 nM of  $K_d$ ; 27-mer SWAP chimera: 56 nM of  $K_d$ ) maintain approximately the same binding affinities as parental R-1 aptamer (54 nM of  $K_d$ ). To determine whether the bound chimera is able to specifically bind and be internalized by BAFF-R expressing cells, we also carried out flow cytometry (Supplementary Figure S3C) and real-time Z-axis confocal microscopy (Figure 4D and F and Supplementary Figure S5B). The Cy3-labelled chimeras selectively bound and were successfully internalized into BAFF-R expressing cells (Jeko-1 and Z138) after 5 h post-treatment. Similar with their parental aptamer R-1, the aptamer–siRNA chimeras were internalized into the cytoplasm of cells (Figure 4F).

Moreover, we performed MTS assays to determine whether our chimeras affect cell proliferation and apoptosis in B-cell line. As shown in Figure 5A, after 48 and 96 h of post-treatment, BAFF ligand induced ~20% proliferation, whereas the chimeras behaved similarly to the parental R-1 aptamer in Jeko-1 cells and showed no increase in cell proliferation. No obvious induction of cell apoptosis was observed in the cells treated with electroporated siRNA, aptamer and chimeras (Figure 5B).

#### BAFF-R aptamer–siRNA chimeras specifically knockdown STAT3 expression levels *via* RNAi pathway

To confirm that the siRNA component was functioning along with the aptamer, after internalization of the BAFF-R aptamer–siRNA chimeras in BAFF-R expressing cells, we also evaluated the relative levels of inhibition of STAT3 expression. Cells were incubated with R-1-STAT3 siRNA chimeras, siRNAs alone, R-1 aptamer and a non-functional control R-1-CCND1 siRNA chimera (targeting cyclin D1). After 2 days of post-treatment, treated cells were harvested, the total RNA was extracted and the expression level of *STAT3* mRNA was determined by qRT-PCR. The R-1-STAT3 siRNA chimeras (27-mer OVH and 27-mer SWAP), but not the aptamers or siRNAs alone, significantly reduced *STAT3* mRNA levels (Supplementary Figure S5C and Figure 6A). The 27-mer OVH chimera exhibited slightly improved potency over the 27-mer SWAP chimera. Importantly, the reduction was B-cell specific, as control cells (CEM human T-cells) treated with either of the

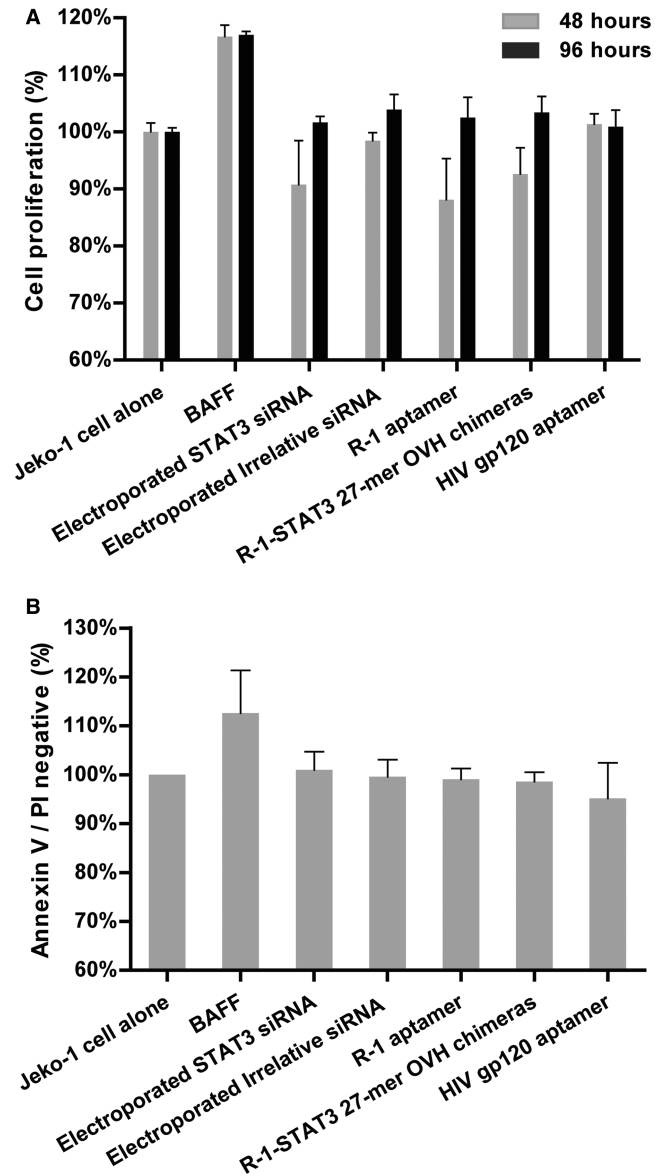


**Figure 5.** Cellular proliferation and apoptosis of aptamer–siRNA chimera-treated NHL cell line. (A) Cell proliferation was assessed 48 or 96 h after the treatment of 400 nM BAFF and RNA. In all, 200 nM STAT3 siRNA was electroporated as a control. BAFF ligand can increase cell proliferation on binding to BAFF-R on Jeko-1 cells. RNA aptamer and its chimeras showed no increase in cell proliferation in Jeko-1. MTS assays were performed, and cell proliferation was calculated in percentage and showed. (B) Cell apoptosis was conducted 96 h after the treatment in Jeko-1 cells. Flow cytometry was performed, and the data were calculated for the percentage of double-negative population of Annexin V and PI staining. Data represent four independent experiments.

R-1-STAT3 siRNA chimeras exhibited no *STAT3* mRNA reduction.

Furthermore, we carried out western blot to detect STAT3 protein levels in Z138 and Jeko-1 (Figure 6B and C and Supplementary Figure S6A) cells as described earlier in the text. As controls, the R-1 aptamer alone and the irrelevant HIV gp120 aptamer were used for both cell lines. To ensure the specificity of the STAT3 siRNA, a non-functional control R-1-CCND1 siRNA chimera was also tested in Z138 cells. Consistent with the qRT-PCR

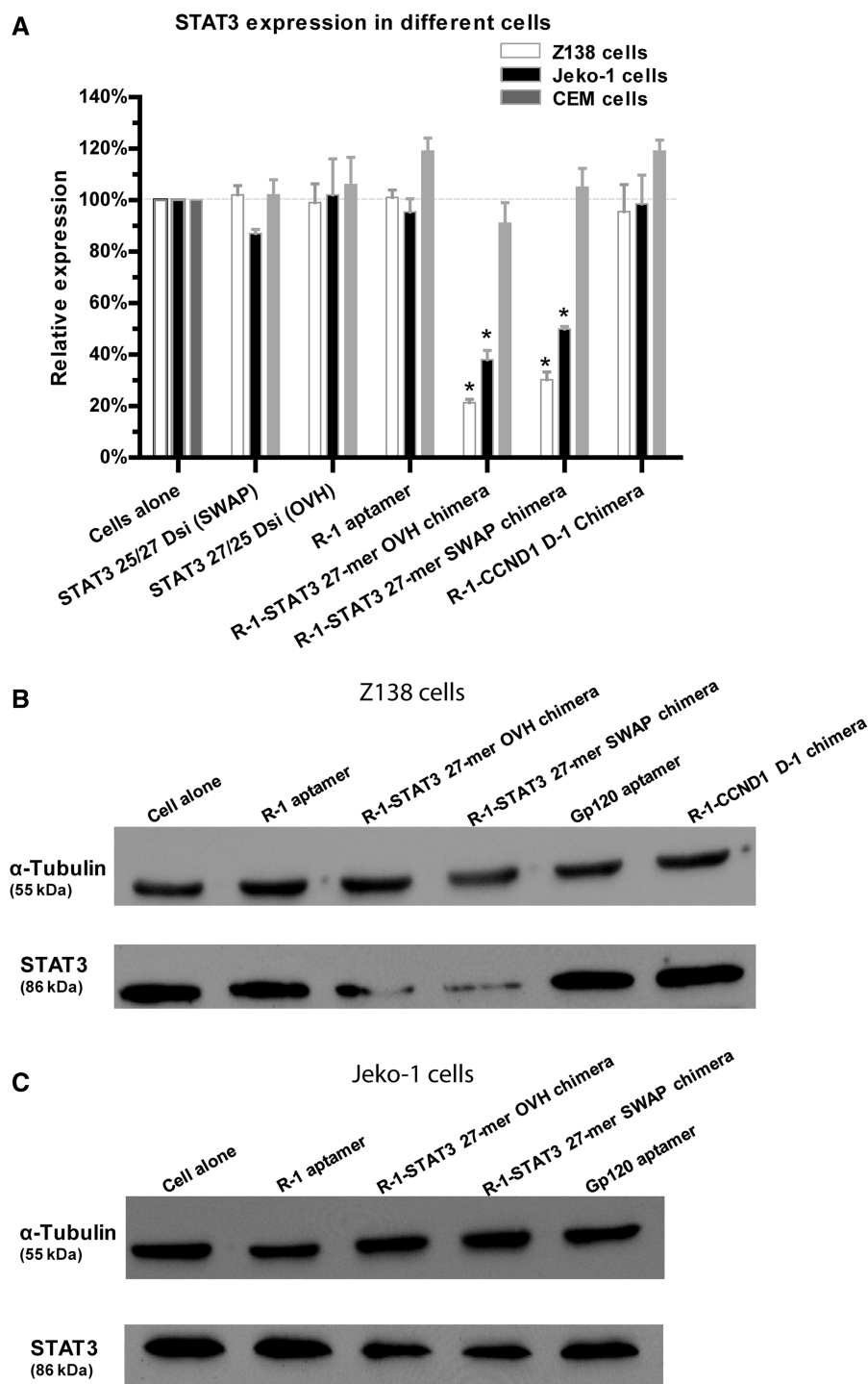


**Figure 6.** Aptamer delivered siRNAs specifically knockdown STAT3 expression. (A) Relative *STAT3* mRNA levels were detected by real-time PCR, with GAPDH as internal control. Jeko-1, Z138 and CEM cells were incubated with BAFF-R aptamers and chimeras. As control siRNA alone, R-1 aptamer, irrelevant aptamer (against gp120) and BAFF-R aptamer–cyclin D1 (CCND1) siRNA chimeras were used. Experiments were performed in triplicate. Asterisk indicates a significant difference compared with control ( $P < 0.01$ , student's *t*-test). STAT3 protein reductions were measured by western blot analysis in Z138 (B) and Jeko-1 (C) cells. Gp120 aptamer and untreated cells served as controls. As loading control,  $\alpha$ -tubulin was used.

data (Figure 6A), only the R-1-STAT3 siRNA chimeras exhibited STAT3 protein reduction in both cell lines (Figure 6B and C).

Additionally, a modified 5'-RACE (rapid amplification of cDNA ends) PCR was performed to ensure RNAi-mediated STAT3 mRNA cleavage (Supplementary

Figure S6B and C). As it has been established that Ago2-mediated cleavage of mRNA between base 10 and 11 relative to the 5'-end of the siRNA guide strand (42,43), the RACE PCR product should display a linker addition at the base 10 nt downstream from the 5'-end of the siRNA guide strand. PCR bands of the predicted

lengths were detected in the total RNAs from Jeko-1 or Z138 cells treated with the chimeras after two nested PCR reactions. No appropriate size products were observed in the non-treated cells or in the siRNA alone-treated cells (Supplementary Figure S6B). The individual clones were sequenced to verify the expected PCR products. Several various cleavage sites were found in the samples treated with the two chimeras. Supplementary Figure S6C indicated the Ago2 cleavage sites and proposed direction of Dicing. For the 27-mer OVH chimera, two major cleavages take place, suggesting that Dicer might bi-directionally enter the DsiRNA to generate different 21- or 22-mer siRNA species. In the case of the 27-mer SWAP chimera, although different cleavage sites were generated, the same direction of Dicer entry was observed, in which Dicer always enters the DsiRNA from 3'-end of antisense strand and generates different siRNA species of various length (19-, 20- or 23-mer siRNAs). The results indicated that the target cleavage sites correlated with Dicer produced siRNAs as revealed by Illumina sequencing (data not shown). These results provide strong evidence that the chimeras-delivered siRNAs are processed intracellular and trigger sequence-specific degradation of the STAT3 target mRNA.

#### **Design and detection of BAFF-R aptamer–stick–siRNA conjugate delivery systems that bind and are internalized by cells expressing BAFF-R**

We previously reported an aptamer–stick–siRNA conjugate for cell-specific siRNA delivery (36), in which aptamer and siRNAs portions are linked *via* a pair of complementary ‘stick’ sequences. As in this design format all the RNA components can be chemically synthesized in a microgram scale, such ‘sticky bridge’ strategy is more feasible for the clinical adaptation of aptamer-mediated siRNA delivery system. As shown in Figure 7A and Supplementary Figure S7A, we designed two R-1 aptamer–stick–STAT3 siRNA conjugates (N-1 and N-2) through swapping sense and antisense strand as previously described (36).

A native gel mobility shift assay was performed to monitor the BAFF-R binding capabilities of the chemically synthesized aptamer, which yielded nanomolar dissociation constant (Supplementary Figure S7B). These synthetic aptamer–stick–siRNA conjugates selectively bind to cells expressing BAFF-R and are internalized into the cytoplasm (Figure 7B and Supplementary Figure S7C), but not into control CEM T-cells (Figure 7C). These live-cell confocal images demonstrated that R-1 aptamer successfully delivers Cy3-labelled siRNA into the cytoplasm of BAFF-R expressing cells. In similarity of their parental R-1 aptamer, these chemically synthetic aptamer (R-1-stick) and aptamer–stick–siRNA conjugates did not increase cell proliferation in Jeko-1 cells (Supplementary Figure S7D). Furthermore, an apoptosis assay was performed with the aptamer and conjugates (Supplementary Figure S7E). These chemical aptamer and conjugates behaved similarly to their T7 transcripts, showing no obvious apoptosis induction.

The function of siRNA portion was confirmed by evaluating the relative expression of target gene STAT3. The cell incubation and qRT–PCR assays were performed as described earlier in the text. Consistent with previous observation of aptamer–siRNA chimeras, only R-1-stick–STAT3 siRNA conjugates (N-1 and N-2) specifically reduced STAT3 mRNA expression in Jeko-1 and Z138 B-cells (Figure 7D), but not in control CEM T-cells (data not shown). For comparison, the N-2 conjugate exhibited slightly stronger potency than N-1. For the N-1 and N-2 conjugates (Figure 7E), Dicer preferentially binds and processes these Dicer substrates from side containing the 2 base 3'-overhang, probably affecting the efficiency of incorporation into RISC and eventually RNAi efficacy (36,44,45).

#### **Chemically synthetic BAFF-R aptamer blocks BAFF ligand-induced activation of SELL**

Additionally, the microarray experiment of total RNAs was performed to explore the interaction of BAFF-R aptamers with the B-cells. BAFF ligand, chemically synthetic BAFF-R aptamer (R-1-stick), the combination of BAFF ligand with R-1-stick and an irrelevant synthetic aptamer control (A-1-stick against HIV-1 gp120) were each incubated with Jeko-1 cells. After 48 h post-treatment, total RNA was isolated and purified for microarray assay. Gene expression profiles were summarized in Supplementary Table S1, indicating the top 10 upregulated genes and their respective fold-changes. Notably, the gene expression profiles were distinct between BAFF ligand treatment and R-1-stick. For example, of these genes, we observed that SELL (selectin-L) (46), also named as LAM-1 encoding a cell surface adhesion molecule that belongs to a family of cell adhesion/homing receptors, was significantly activated (fold-change = 8.3) with BAFF ligand treatment. SELL gene product is required for binding and subsequent rolling of leucocytes on endothelial cells, facilitating their migration into secondary lymphoid organs and inflammation sites (46). Recent evidence indicates that selectin-mediated interactions may contribute to formation of a permissive microenvironment for metastasis (47). In particular, selectin-L mediates the recruitment of leucocytes to cancer cells, and the absence of selectin-L leads to attenuation of metastasis (48). Therefore, a significant increase of SELL level in Jeko-1 cells suggests that the interaction of BAFF ligand and BAFF receptor on the B-cell surface may play an important role in selectin-L-mediated metastasis of leucocytes. In contrast, BAFF-R aptamer (R-1-stick) only showed a slight increase of SELL gene level (fold-change = 1.7), implying a different pathway between aptamer and B-cells.

To validate this observation in microarray analysis, the same total RNA samples were assayed for SELL gene expression *via* qRT–PCR. As shown in Figure 8, BAFF ligand dramatically upregulated SELL expression, whereas no significant activation of SELL level was observed in R-1-stick treatment. Interestingly, when the combination of BAFF ligand with R-1-stick was applied, no increase in SELL expression was detected, which suggested that BAFF-R aptamer may counteract

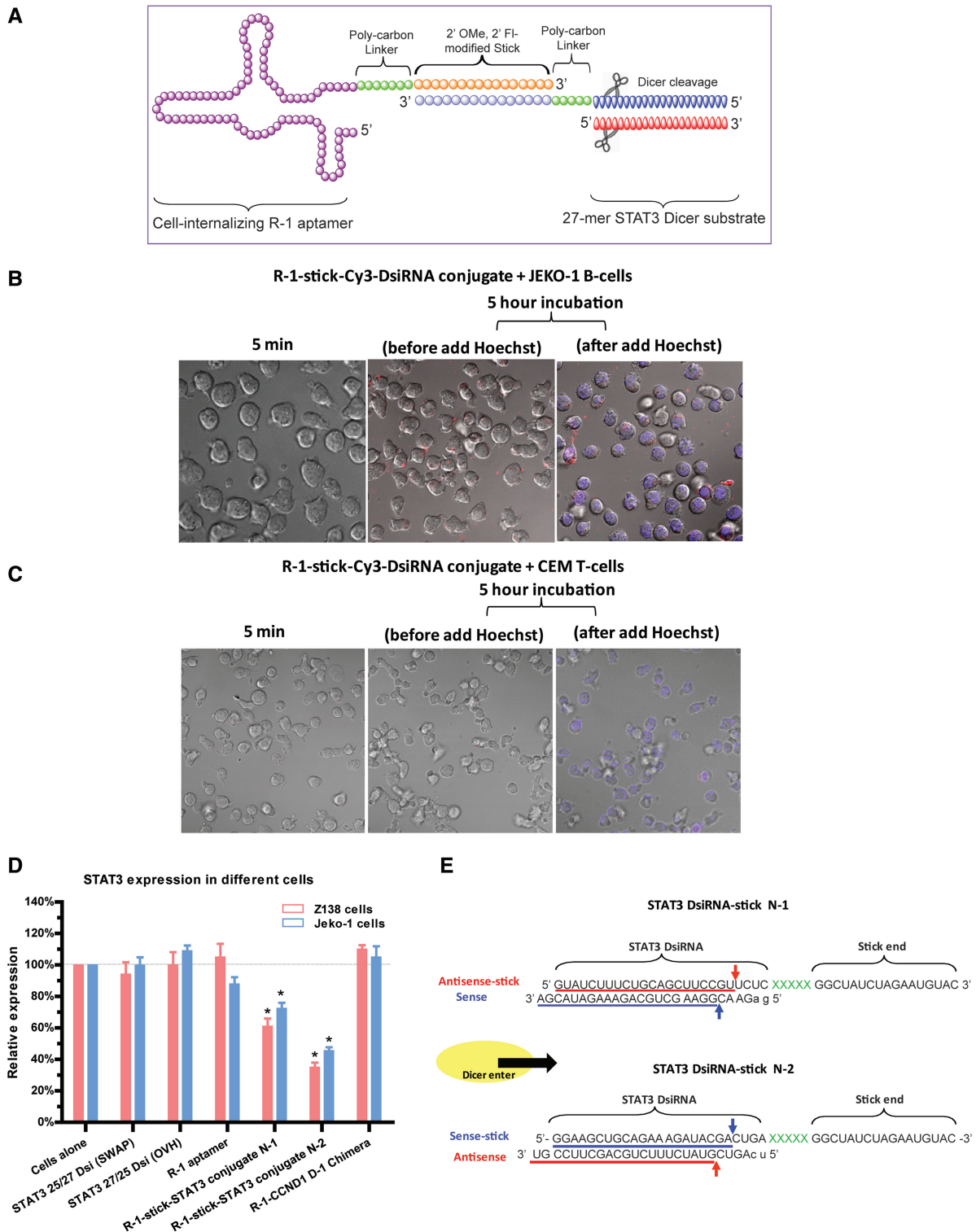


**Figure 7.** Cell-type-specific aptamer-stick-siRNA conjugates delivery system. (A) Schematic aptamer-stick-siRNA conjugates: the region of the BAFF-R aptamer is responsible for binding to BAFF-R, and the siRNA is targeting STAT3 gene. The DsiRNA is linked to the aptamer portion via the 'stick' sequence that consists of 16 nt appended to the aptamer 3'-end, allowing complementary interaction of one of the two siRNA strands with the aptamer. A linker of seven three-carbons between the aptamer RNA and the stick portion is used to avoid steric interaction of the stick with the aptamer. Two versions, N-1 and N-2, were designed, in which DsiRNA orientation is different. (B and C) Internalization and intracellular localization study. Jeko-1 (B) or CEM control cells (C) were grown in 35-mm plates and incubated in culture medium with 60 nM concentration of conjugate N-1 containing a 5'-Cy3-labelled sense strand for real-time live-cell confocal microscopy analysis as previously described. The conjugate showed cell-type-specific binding affinity. (D) Aptamer-delivered siRNAs specifically knockdown STAT3 expression. Relative *STAT3* mRNA levels were detected by RT-PCR, with *GAPDH* as internal control. Jeko-1 and Z138 cells were incubated with BAFF-R aptamers and conjugates. Experiments were performed in triplicate. Double asterisks indicate a significant difference compared with control ( $P < 0.01$ , student's *t*-test). (E) Schematic Dicer processing of aptamer-stick-siRNA conjugates N-1 and N-2 and resulting in siRNA products. As shown by black arrows, Dicer preferentially binds and processes these Dicer substrates from side containing the 2 base 3'-overhang.

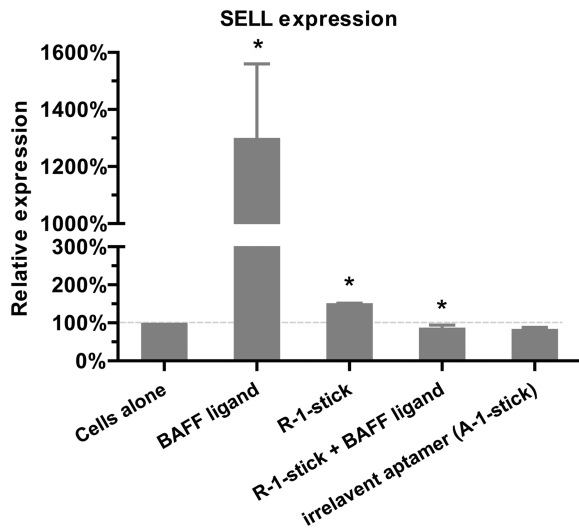


**Figure 8.** SELL expression by qRT-PCR. BAFF ligand, chemically synthetic BAFF-R aptamer (R-1-stick), the combination of BAFF ligand with R-1-stick and an irrelevant synthetic aptamer control (A-1-stick against HIV-1 gp120) were incubated with Jeko-1 cells, respectively. After 48 h post-treatment, total RNAs were isolated and purified for qRT-PCR analysis. Human large ribosomal protein (RPLPO) expression was used as an internal control for data normalization. Experiments were performed in triplicate. Asterisk indicates a significant difference compared with control ( $P < 0.05$ , student's *t*-test).

the effect induced by BAFF ligand and block BAFF ligand-mediated SELL activation.

## DISCUSSION

Macugen (pegaptanib) was the first aptamer approved by the FDA for the treatment of wet age-related macular degeneration (49). Since then, aptamers with low-binding affinities have been used for various diseases and flexible applications as new potential drugs and delivery vehicles (32,50). Aptamers that target specific cell-surface proteins are often used for molecule delivery to specific target cell types, such as tumour-cells (33,34), thereby reducing off-target effects or unwanted other side effects. In this regard, we generated BAFF-R RNA aptamers with nanomolar binding affinity, which are able to deliver siRNAs efficiently to NHL cell lines without increasing cell proliferation or survival of cancerous cells. In a therapeutic setting, multiple aptamers and siRNAs might be needed to inhibit or kill cancer cells completely as in most cancers more than one gene is deregulated. Therefore, the BAFF-R aptamers illustrate dual function: inhibition of proliferation and survival mediated by BAFF and siRNA delivery vehicle.

In the present work, we isolated 2'-fluoro-modified RNA aptamers *via in vitro* SELEX that bind specifically to BAFF-R from an 81-nt RNA library. Our results showed specific binding and internalization of our aptamers to BAFF-R expressing B-cell lymphoma cells but not BAFF-R-negative T-cells (CEM). We observed an aggregation of aptamer or aptamer-siRNA conjugates in the cytoplasm by real-time confocal microscopy, suggesting that aptamers are internalized probably by

receptor-mediated endocytosis. Although the details of endosomal escape remain unclear, the specific downregulation of target genes mediated by the aptamer-siRNA conjugates suggests that siRNA can be released from endosome and enter RNAi pathway. We designed two BAFF-R aptamer-STAT3 DsiRNA conjugates, one is aptamer-siRNA chimera and another is aptamer-stick-siRNA conjugate. Both conjugates were successfully processed by Dicer and triggered specific mRNA cleavage in B-cells, leading to similar levels of target mRNA and protein reduction.

In addition, it was known that BAFF stimulates survival of B-cells on binding to BAFF-R (8,9) and enhances NHL B-cell proliferation especially in combination with APRIL (11). Furthermore, peripheral blood mature B-cells from mice overexpressing BAFF have an increase of Bcl-2 protein expression (51), which at least in part accounts for their enhanced survival. Moreover, total RNA microarray analysis also showed BAFF significantly upregulates selectin-L expression, which contributes to formation of a permissive microenvironment for metastasis. These findings raised concerns that our BAFF-R aptamers might have the unwanted side effect of increasing survival and proliferation of B-cells and either cause cancer or help the cancerous cells to survive. However, no increase in cell proliferation could be detected with the aptamers or the conjugates derived from R-1. Indeed the aptamers even blocked ligand-mediated proliferation in NHL cell lines most probably by competing for the receptor. Furthermore, our results that BAFF-R aptamer counteracts BAFF ligand-mediated SELL activation imply a potential use of BAFF-R aptamers in blocking SELL-mediated metastasis of B-cells. Therefore, BAFF-R aptamers show potential as a therapeutic by itself for NHL or autoimmune disease and not exclusively as delivery vehicle.

In the present study, STAT3 siRNA was used as proof of principle to show successful delivery as well as specific gene silencing in B-cells. Although silencing of STAT3 had no effect on cell proliferation or apoptosis (Figure 5A and B), the aptamer-STAT3 siRNA chimeras did not indicate a negative effect on the binding to BAFF-R (Figure 5), whereas BAFF enhanced proliferation. The mechanism underlying the oncogenic potential of STAT3 is not entirely understood. Constitutively active STAT3 contributes to tumour progression *via* various mechanisms (52) and associates with multiple factors to play roles in cell proliferation and survival (27,53). Knockdown of only one of these factors (such as STAT3) by 50–80%, (Supplementary Figure S5C) has only little effect on the cell survival and proliferation. Cells can easily compensate for a reduction such as this either by increasing expression of other proteins or by upregulating other pathways. Moreover, it was found that the activated/phosphorylated forms of STAT3 in MCL tumours contributed to the pathogenesis of MCL (53–55). Although MCL cell lines showed a high level of the inactive form of STAT3, the presence of the activated form (phosphorylated form) was not detectable in some MCL cells (such as Jeko-1, MINO and GRANTA) (29) because of their use of alternative pathway to achieve proliferative and survival signals. It

has been demonstrated that silencing cyclin D1 (CCND1, a known cell cycle regulator whose overexpression is a hallmark of MCL) by 40–60% had no anti-proliferative effect (56). However, the combination of siRNA-mediated inhibition of the cyclins along with etoposide and doxorubicin could decrease the doses of chemotherapeutic agents as well as enhance cell apoptosis. Nevertheless, the reduction of STAT3 may make the cells more susceptible to chemotherapy agents or other treatments, therefore, probably improving their therapeutic index.

Our aptamer–siRNA conjugates have the advantage over antibody by not only competing BAFF for binding to BAFF-R but also delivering a wide range of therapeutics, such as various siRNAs (which we tested here), and toxins or chemotherapeutics could be delivered directly to B-cells. Previously, it was successfully demonstrated that an anti-Prostate-specific membrane antigen (PSMA) RNA aptamer conjugated to the toxin gelonin showed enhanced efficacy in treatment of prostate cancer and decreased toxicity on cells not expressing PSMA (57). Furthermore, chimeric proteins composed of chemokine ligands, such as interleukin-2, -3 or vascular endothelial growth factor, fused to various toxins (e.g. gelonin, diphtheria) and exhibited significant and selective cytotoxic effects against target cells with nanomolar affinity. Recently, gelonin was also fused to BAFF (rGel/BLys) (5) and indicated the highest cytotoxicity on MCL cell lines (6). Biodistribution of rGel/BLys in Severe combined immunodeficiency (SCID) mice showed localization in tumour and reduction of tumour growth (58). Nevertheless, the heterogeneous intratumoural distribution made the eradication of the solid tumour by treatment with rGel/BLys alone impossible (58). All these studies taken together indicate that a combination of two or more separate therapeutics such as an antibody/aptamer combined with a toxin/siRNA might provide enhanced effects. With the technological maturation and increasing knowledge of RNAi and aptamers, it seems logical to partner the two kinds of therapeutic nucleic acids for expanding the options for targeted RNAi. To this end, our aptamer–siRNA conjugates are a step into the right direction in combining effective therapeutics against NHL together to result in a more effective therapeutic.

In summary, we demonstrated that the BAFF-R aptamers not only act as specific delivery vehicles of siRNAs or potential other molecules but also in itself could be used as potential therapeutic for NHL by blocking ligand-mediated proliferation and survival signals.

## SUPPLEMENTARY DATA

Supplementary Data are available at NAR Online: Supplementary Table 1, Supplementary Figures 1–7 and Supplementary Methods.

## ACKNOWLEDGEMENTS

The authors thank Britta Vallazza for helping them with the design of the RNA-library and primers and helpful discussions. Furthermore, they thank Brooke

Seidemantle and Anja Honegger for helping to produce aptamers. They thank Dr Marcin Kortylewski for providing them the sequences of human STAT3 DsiRNA and primers of qRT–PCR. J.Z., K.T. and J.J.R. conceived and designed experiments. J.Z., K.T. and J.B. wrote the manuscript. J.Z. isolated/characterized BAFF-R aptamers and designed and tested aptamer–siRNA conjugates. K.T. performed MTS assay and competition assay of aptamers and western blot. P.C. prepared total RNAs for microarray assay and conducted MTS assay of synthetic aptamer and conjugates. J.A. performed SELL qRT–PCR assay. S.F. advised the target mRNAs and cell lines for testing. R.C. collected patient samples for B-cell isolation. P.S. synthesized siRNA and aptamers-stick. X. Z. did 5'-<sup>32</sup>P labelling.

## FUNDING

Nesvig Lymphoma Foundation; Think Cure; Keck Foundation; National Institutes of Health (NIH) [2P50CA107399 to J.J.R. and S.F., R37AI029329 to J.J.R.]; NCI K12 Calabresi Career Development Award to R.C. Funding for open access charge: NIH.

*Conflict of interest statement.* J.J.R. and J.Z. have an issued patent entitled 'Cell-type-specific aptamer-siRNA delivery system for HIV-1 therapy'. USPTO, No. US 8, 222, 226 B2, issued date: 17 July 2012. J.J.R., J. Z. and K.T. have a patent pending on 'RNA aptamers against BAFF-R as cell-type-specific delivery agents and methods for their use', The United States Patent, application number: US2011/032385, Publication date: 20 Oct 2011.

## REFERENCES

- Thompson, J.S., Bixler, S.A., Qian, F., Vora, K., Scott, M.L., Cachero, T.G., Hession, C., Schneider, P., Sizing, I.D., Mullen, C. *et al.* (2001) BAFF-R, a newly identified TNF receptor that specifically interacts with BAFF. *Science*, **293**, 2108–2111.
- Moore, P.A., Belvedere, O., Orr, A., Pieri, K., LaFleur, D.W., Feng, P., Soppet, D., Charters, M., Gentz, R., Parmelee, D. *et al.* (1999) BLYS: member of the tumor necrosis factor family and a B lymphocyte stimulator. *Science*, **285**, 260–263.
- Gross, J.A., Johnston, J., Mudri, S., Enselman, R., Dillon, S.R., Madden, K., Xu, W., Parrish-Novak, J., Foster, D., Lofton-Day, C. *et al.* (2000) TACI and BCMA are receptors for a TNF homologue implicated in B-cell autoimmune disease. *Nature*, **404**, 995–999.
- Craxton, A., Magaletti, D., Ryan, E.J. and Clark, E.A. (2003) Macrophage- and dendritic cell-dependent regulation of human B-cell proliferation requires the TNF family ligand BAFF. *Blood*, **101**, 4464–4471.
- Nimmanapalli, R., Lyu, M.A., Du, M., Keating, M.J., Rosenblum, M.G. and Gandhi, V. (2007) The growth factor fusion construct containing B-lymphocyte stimulator (BLYS) and the toxin rGel induces apoptosis specifically in BAFF-R-positive CLL cells. *Blood*, **109**, 2557–2564.
- Lyu, M.A., Cheung, L.H., Hittelman, W.N., Marks, J.W., Aguiar, R.C. and Rosenblum, M.G. (2007) The rGel/BLYS fusion toxin specifically targets malignant B-cells expressing the BLYS receptors BAFF-R, TACI, and BCMA. *Mol. Cancer Ther.*, **6**, 460–470.
- Shulga-Morskaya, S., Dobles, M., Walsh, M.E., Ng, L.G., MacKay, F., Rao, S.P., Kalled, S.L. and Scott, M.L. (2004) B-cell-activating factor belonging to the TNF family acts through

- separate receptors to support B-cell survival and T cell-independent antibody formation. *J. Immunol.*, **173**, 2331–2341.
8. Thompson, J.S., Schneider, P., Kalled, S.L., Wang, L., Lefevre, E.A., Cachero, T.G., MacKay, F., Bixler, S.A., Zafari, M., Liu, Z.Y. *et al.* (2000) BAFF binds to the tumor necrosis factor receptor-like molecule B-cell maturation antigen and is important for maintaining the peripheral B-cell population. *J. Exp. Med.*, **192**, 129–135.
  9. Batten, M., Groom, J., Cachero, T.G., Qian, F., Schneider, P., Tschopp, J., Browning, J.L. and Mackay, F. (2000) BAFF mediates survival of peripheral immature B lymphocytes. *J. Exp. Med.*, **192**, 1453–1466.
  10. Ju, Z.L., Shi, G.Y., Zuo, J.X. and Zhang, J.W. (2007) Unexpected development of autoimmunity in BAFF-R-mutant MRL-lpr mice. *Immunology*, **120**, 281–289.
  11. He, B., Chadburn, A., Jou, E., Schattner, E.J., Knowles, D.M. and Cerutti, A. (2004) Lymphoma B-cells evade apoptosis through the TNF family members BAFF/BLyS and APRIL. *J. Immunol.*, **172**, 3268–3279.
  12. Novak, A.J., Grote, D.M., Stenson, M., Ziesmer, S.C., Witzig, T.E., Habermann, T.M., Harder, B., Ristow, K.M., Bram, R.J., Jelinek, D.F. *et al.* (2004) Expression of BLyS and its receptors in B-cell non-Hodgkin lymphoma: correlation with disease activity and patient outcome. *Blood*, **104**, 2247–2253.
  13. Kern, C., Cornuel, J.F., Billard, C., Tang, R., Rouillard, D., Stenou, V., Defrance, T., Ajchenbaum-Cymbalista, F., Simonin, P.Y., Feldblum, S. *et al.* (2004) Involvement of BAFF and APRIL in the resistance to apoptosis of B-CLL through an autocrine pathway. *Blood*, **103**, 679–688.
  14. Tecchio, C., Nadali, G., Scapini, P., Bonetto, C., Visco, C., Tamassia, N., Vassilakopoulos, T.P., Pangalis, G.A., Calzetti, F., Nardelli, B. *et al.* (2007) High serum levels of B-lymphocyte stimulator are associated with clinical-pathological features and outcome in classical Hodgkin lymphoma. *Br. J. Haematol.*, **137**, 553–559.
  15. Siegel, R., Naishadham, D. and Jemal, A. (2012) Cancer statistics, 2012. *CA Cancer J. Clin.*, **62**, 10–29.
  16. Mackay, F. and Schneider, P. (2009) Cracking the BAFF code. *Nat. Rev. Immunol.*, **9**, 491–502.
  17. Friedberg, J.W. and Fisher, R.I. (2008) Diffuse large B-cell lymphoma. *Hematol. Oncol. Clin. North Am.*, **22**, 941–952, ix.
  18. Coiffier, B. (2005) Current strategies for the treatment of diffuse large B-cell lymphoma. *Curr. Opin. Hematol.*, **12**, 259–265.
  19. Feugier, P., Van Hoof, A., Sebban, C., Solal-Celigny, P., Bouabdallah, R., Ferme, C., Christian, B., Lepage, E., Tilly, H., Morschhauser, F. *et al.* (2005) Long-term results of the R-CHOP study in the treatment of elderly patients with diffuse large B-cell lymphoma: a study by the Groupe d'Etude des Lymphomes de l'Adulte. *J. Clin. Oncol.*, **23**, 4117–4126.
  20. Friedberg, J.W. and Fisher, R.I. (2006) Diffuse large B-cell NHL. *Cancer Treat. Res.*, **131**, 121–140.
  21. Campo, E., Raffeld, M. and Jaffe, E.S. (1999) Mantle-cell lymphoma. *Semin. Hematol.*, **36**, 115–127.
  22. Nakamura, N., Hase, H., Sakurai, D., Yoshida, S., Abe, M., Tsukada, N., Takizawa, J., Aoki, S., Kojima, M., Nakamura, S. *et al.* (2005) Expression of BAFF-R (BR 3) in normal and neoplastic lymphoid tissues characterized with a newly developed monoclonal antibody. *Virchows Arch.*, **447**, 53–60.
  23. Monti, S., Savage, K.J., Kutok, J.L., Feuerhake, F., Kurtin, P., Mihm, M., Wu, B., Pasqualucci, L., Neuberg, D., Aguiar, R.C. *et al.* (2005) Molecular profiling of diffuse large B-cell lymphoma identifies robust subtypes including one characterized by host inflammatory response. *Blood*, **105**, 1851–1861.
  24. Shaffer, A.L., Wright, G., Yang, L., Powell, J., Ngo, V., Lamy, L., Lam, L.T., Davis, R.E. and Staudt, L.M. (2006) A library of gene expression signatures to illuminate normal and pathological lymphoid biology. *Immunol. Rev.*, **210**, 67–85.
  25. Kuppers, R. (2005) Mechanisms of B-cell lymphoma pathogenesis. *Nat. Rev. Cancer*, **5**, 251–262.
  26. Yu, H. and Jove, R. (2004) The STATs of cancer—new molecular targets come of age. *Nat. Rev. Cancer*, **4**, 97–105.
  27. Yu, H., Pardoll, D. and Jove, R. (2009) STATs in cancer inflammation and immunity: a leading role for STAT3. *Nat. Rev. Cancer*, **9**, 798–809.
  28. Ding, B.B., Yu, J.J., Yu, R.Y., Mendez, L.M., Shakhovich, R., Zhang, Y., Cattoretti, G. and Ye, B.H. (2008) Constitutively activated STAT3 promotes cell proliferation and survival in the activated B-cell subtype of diffuse large B-cell lymphomas. *Blood*, **111**, 1515–1523.
  29. Lai, R., Rassidakis, G.Z., Medeiros, L.J., Leventaki, V., Keating, M. and McDonnell, T.J. (2003) Expression of STAT3 and its phosphorylated forms in mantle cell lymphoma cell lines and tumours. *J. Pathol.*, **199**, 84–89.
  30. Do, R.K., Hatada, E., Lee, H., Tourigny, M.R., Hilbert, D. and Chen-Kiang, S. (2000) Attenuation of apoptosis underlies B lymphocyte stimulator enhancement of humoral immune response. *J. Exp. Med.*, **192**, 953–964.
  31. Khare, S.D., Sarosi, I., Xia, X.Z., McCabe, S., Miner, K., Solovyev, I., Hawkins, N., Kelley, M., Chang, D., Van, G. *et al.* (2000) Severe B-cell hyperplasia and autoimmune disease in TALL-1 transgenic mice. *Proc. Natl Acad. Sci. USA*, **97**, 3370–3375.
  32. Zhou, J. and Rossi, J.J. (2009) The therapeutic potential of cell-internalizing aptamers. *Curr. Top Med. Chem.*, **9**, 1144–1157.
  33. Zhou, J., Li, H., Li, S., Zaia, J. and Rossi, J.J. (2008) Novel dual inhibitory function aptamer-siRNA delivery system for HIV-1 therapy. *Mol. Ther.*, **16**, 1481–1489.
  34. McNamara, J.O. II, Andreckek, E.R., Wang, Y., Viles, K.D., Rempel, R.E., Gilboa, E., Sullenger, B.A. and Giangrande, P.H. (2006) Cell type-specific delivery of siRNAs with aptamer-siRNA chimeras. *Nat. Biotechnol.*, **24**, 1005–1015.
  35. Briones, J., Timmerman, J.M., Hilbert, D.M. and Levy, R. (2002) BLyS and BLyS receptor expression in non-Hodgkin's lymphoma. *Exp. Hematol.*, **30**, 135–141.
  36. Zhou, J., Swiderski, P., Li, H., Zhang, J., Neff, C.P., Akkina, R. and Rossi, J.J. (2009) Selection, characterization and application of new RNA HIV gp 120 aptamers for facile delivery of Dicer substrate siRNAs into HIV infected cells. *Nucleic Acids Res.*, **37**, 3094–3109.
  37. Tuerk, C. and Gold, L. (1990) Systematic evolution of ligands by exponential enrichment: RNA ligands to bacteriophage T4 DNA polymerase. *Science*, **249**, 505–510.
  38. Fu, L., Lin-Lee, Y.C., Pham, L.V., Tamayo, A.T., Yoshimura, L.C. and Ford, R.J. (2009) BAFF-R promotes cell proliferation and survival through interaction with IKKbeta and NF-kappaB/c-Rel in the nucleus of normal and neoplastic B-lymphoid cells. *Blood*, **113**, 4627–4636.
  39. Kortylewski, M. and Yu, H. (2008) Role of Stat3 in suppressing anti-tumor immunity. *Curr. Opin. Immunol.*, **20**, 228–233.
  40. Bowman, T., Garcia, R., Turkson, J. and Jove, R. (2000) STATs in oncogenesis. *Oncogene*, **19**, 2474–2488.
  41. Dassie, J.P., Liu, X.Y., Thomas, G.S., Whitaker, R.M., Thiel, K.W., Stockdale, K.R., Meyerholz, D.K., McCaffrey, A.P., McNamara, J.O. II and Giangrande, P.H. (2009) Systemic administration of optimized aptamer-siRNA chimeras promotes regression of PSMA-expressing tumors. *Nat. Biotechnol.*, **27**, 839–849.
  42. Matranga, C., Tomari, Y., Shin, C., Bartel, D.P. and Zamore, P.D. (2005) Passenger-strand cleavage facilitates assembly of siRNA into Ago2-containing RNAi enzyme complexes. *Cell*, **123**, 607–620.
  43. Meister, G., Landthaler, M., Patkaniowska, A., Dorsett, Y., Teng, G. and Tuschl, T. (2004) Human Argonaute2 mediates RNA cleavage targeted by miRNAs and siRNAs. *Mol. Cell*, **15**, 185–197.
  44. Zhou, J., Song, M.S., Jacobi, A.M., Behlke, M.A., Wu, X. and Rossi, J.J. (2012) Deep Sequencing Analyses of DsiRNAs Reveal the Influence of 3' Terminal Overhangs on Dicing Polarity, Strand Selectivity, and RNA Editing of siRNAs. *Mol. Ther.*, **1**, e17.
  45. Zhou, J., Neff, C.P., Swiderski, P., Li, H., Smith, D.D., Aboellail, T., Remling-Mulder, L., Akkina, R. and Rossi, J.J. (2013) Functional *in vivo* delivery of multiplexed anti-HIV-1 siRNAs via a chemically synthesized aptamer with a sticky bridge. *Mol. Ther.*, **21**, 192–200.
  46. Laubli, H. and Borsig, L. (2010) Selectins promote tumor metastasis. *Semin Cancer Biol*, **20**, 169–177.
  47. Laubli, H., Spanaus, K.S. and Borsig, L. (2009) Selectin-mediated activation of endothelial cells induces expression of CCL5 and

- promotes metastasis through recruitment of monocytes. *Blood*, **114**, 4583–4591.
48. Kneuer,C., Ehrhardt,C., Radomski,M.W. and Bakowsky,U. (2006) Selectins–potential pharmacological targets? *Drug Discov. Today*, **11**, 1034–1040.
  49. Ng,E.W., Shima,D.T., Calias,P., Cunningham,E.T. Jr, Guyer,D.R. and Adamis,A.P. (2006) Pegaptanib, a targeted anti-VEGF aptamer for ocular vascular disease. *Nat. Rev. Drug Discov.*, **5**, 123–132.
  50. Zhou,J. and Rossi,J.J. Aptamer-targeted cell-specific RNA interference. *Silence*, **1**, 4.
  51. Mackay,F., Woodcock,S.A., Lawton,P., Ambrose,C., Baetscher,M., Schneider,P., Tschopp,J. and Browning,J.L. (1999) Mice transgenic for BAFF develop lymphocytic disorders along with autoimmune manifestations. *J. Exp. Med.*, **190**, 1697–1710.
  52. Bromberg,J.F., Wrzeszczynska,M.H., Devgan,G., Zhao,Y., Pestell,R.G., Albanese,C. and Darnell,J.E. Jr (1999) Stat3 as an oncogene. *Cell*, **98**, 295–303.
  53. Campbell,C.L., Jiang,Z., Savarese,D.M. and Savarese,T.M. (2001) Increased expression of the interleukin-11 receptor and evidence of STAT3 activation in prostate carcinoma. *Am. J. Pathol.*, **158**, 25–32.
  54. Gouilleux-Gruart,V., Gouilleux,F., Desaint,C., Claisse,J.F., Capiod,J.C., Delobel,J., Weber-Nordt,R., Dusanter-Fourt,I., Dreyfus,F., Groner,B. *et al.* (1996) STAT-related transcription factors are constitutively activated in peripheral blood cells from acute leukemia patients. *Blood*, **87**, 1692–1697.
  55. Kube,D., Holtick,U., Vockerodt,M., Ahmadi,T., Haier,B., Behrmann,I., Heinrich,P.C., Diehl,V. and Tesch,H. (2001) STAT3 is constitutively activated in Hodgkin cell lines. *Blood*, **98**, 762–770.
  56. Tiemann,K., Alluin,J.V., Honegger,A., Chomchan,P., Gaur,S., Yun,Y., Forman,S.J., Rossi,J.J. and Chen,R.W. (2011) Small interfering RNAs targeting cyclin D1 and cyclin D2 enhance the cytotoxicity of chemotherapeutic agents in mantle cell lymphoma cell lines. *Leuk Lymphoma*, **52**, 2148–2154.
  57. Chu,T.C., Marks,J.W. III, Lavery,L.A., Faulkner,S., Rosenblum,M.G., Ellington,A.D. and Levy,M. (2006) Aptamer:toxin conjugates that specifically target prostate tumor cells. *Cancer Res.*, **66**, 5989–5992.
  58. Wen,X., Lyu,M.A., Zhang,R., Lu,W., Huang,Q., Liang,D., Rosenblum,M.G. and Li,C. (2011) Biodistribution, pharmacokinetics, and nuclear imaging studies of (111)in-labeled rGel/BLyS fusion toxin in SCID mice bearing B-cell lymphoma. *Mol. Imaging Biol.*, **13**, 721–729.